Metal-chelating peptides separation using immobilized metal ion affinity chromatography : experimental methodology and simulation

Rachel Irankunda, Jairo Andrés Camaño Echavarría, Cédric Paris, Loïc Stefan, Stéphane Desobry, Katalin Selmeczi, Laurence Muhr, Laetitia Canabady-Rochelle

separations

MDPI

Review

Metal-Chelating Peptides Separation Using Immobilized Metal Ion Affinity Chromatography: Experimental Methodology and Simulation

Rachel Irankunda [1,*], Jairo Andrés Camaño Echavarría [1], Cédric Paris [2], Loïc Stefan [3], Stéphane Desobry [2], Katalin Selmeczi [4], Laurence Muhr [1] and Laetitia Canabady-Rochelle [1,*]

[1] Université de Lorraine, CNRS, LRGP, F-54000 Nancy, France
[2] Université de Lorraine, LIBIO, F-54000 Nancy, France
[3] Université de Lorraine, CNRS, LCPM, F-54000 Nancy, France
[4] Université de Lorraine, CNRS, L2CM, F-54000 Nancy, France
* Correspondence: rachel.irankunda@univ-lorraine.fr (R.I.); laetitia.canabady-rochelle@univ-lorraine.fr (L.C.-R.); Tel.: +33-(0)3-7274-3886 (L.C.-R.)

Abstract: Metal-Chelating Peptides (MCPs), obtained from protein hydrolysates, present various applications in the field of nutrition, pharmacy, cosmetic etc. The separation of MCPs from hydrolysates mixture is challenging, yet, techniques based on peptide-metal ion interactions such as Immobilized Metal Ion Affinity Chromatography (IMAC) seem to be efficient. However, separation processes are time consuming and expensive, therefore separation prediction using chromatography modelling and simulation should be necessary. Meanwhile, the obtention of sorption isotherm for chromatography modelling is a crucial step. Thus, Surface Plasmon Resonance (SPR), a biosensor method efficient to screen MCPs in hydrolysates and with similarities to IMAC might be a good option to acquire sorption isotherm. This review highlights IMAC experimental methodology to separate MCPs and how, IMAC chromatography can be modelled using transport dispersive model and input data obtained from SPR for peptides separation simulation.

Keywords: chromatography modelling; complexation; IMAC; peptide; SPR; separation; simulation

Citation: Irankunda, R.; Camaño Echavarría, J.A.; Paris, C.; Stefan, L.; Desobry, S.; Selmeczi, K.; Muhr, L.; Canabady-Rochelle, L. Metal-Chelating Peptides Separation Using Immobilized Metal Ion Affinity Chromatography: Experimental Methodology and Simulation. *Separations* **2022**, *9*, 370. https://doi.org/10.3390/separations9110370

Academic Editor: Rosa María Alonso

Received: 30 September 2022
Accepted: 10 November 2022
Published: 14 November 2022

1. Introduction

Hydrolysates are complex mixtures of various bioactive peptides which are obtained from the enzymatic hydrolysis of animal or plant proteins including co-products [1]. They have been reported as antioxidant, antihypertensives, anti-inflammatory, antimicrobial, metal-chelators [2–4]. Metal-Chelating Peptides (MCPs) are present in that former mixture, and they are peptides endowed with the capacity to complex metal ion. Therefore, this property confer them the ability to be used in various domains such as nutrition, pharmacy, health, cosmetic and separation processes [1]. However, the separation of peptides is challenging due to their low concentration in hydrolysates (i.e., complex mixtures of peptides). Up until now, the empirical approach used for their discovery was based on many cycles of separation/fractionation and subsequent biological tests to identify the bioactive peptide(s) of interest. Generally, various types of chromatography can be used to perform the separation and purification of peptides such as immobilized metal ion affinity chromatography (IMAC), ion exchange chromatography (IEC), gel filtration chromatography (GFC), reverse phase—high performance liquid chromatography (RP-HPLC) or reverse phase—ultra performance liquid chromatography (RP-UPLC)[1]. It has been demonstrated that IMAC exhibits some advantages compared to other types of chromatography due to its high selectivity for metal-chelating molecules, complete regeneration of column, high binding capacity and high recovery, since the condition used for eluting molecules are non-denaturing [1,5,6]. In addition, its high specificity allows

for the separation of peptides that are particularly chelators of a specific metal ion, which is immobilized in the column; this is the reason why we selected IMAC to study as an efficient technique for MCPs separation.

However, the separation and purification of peptides can be time consuming, expensive and uncertain. Hence, chromatography modelling and simulation can be used for predicting separation. Generally, transport dispersive model and cascade of continuous stirred-tank reactors model can be used for designing liquid chromatography separation. Furthermore, the knowledge of sorption isotherms is important for simulating chromatography separation, and they can be determined by static methods such as batch, adsorption-desorption or dynamic methods such as frontal analysis, perturbation, dispersed front analysis and chromatogram fitting [7,8]. However, these methods require a significant amount of sample and experimental effort. Given that the samples usually investigated in chromatography separation are expensive (e.g., therapeutic proteins, peptides), novel approaches to determine sorption isotherm were developed, such as direct inverse method [9], microfluidic chip approach [10] and modern biosensors methods such as SPR and quartz crystal microbalance [11].

Therefore, the aim of this review is to report and discuss an alternative method (Figure 1a) simulating the MCPs separation in IMAC by using a transport dispersive model and peptides binding affinity data obtained from Surface Plasmon Resonance (SPR), considering SPR-IMAC analogy (Figure 1b). Indeed, SPR is highly sensitive for screening MCPs in hydrolysates [12], it requires small amount of samples and buffers and it is a technique which presents analogies to IMAC (same immobilized metal ion, same complexing agent). Thus, SPR technique will be used to determine sorption isotherm for further chromatography modelling and simulation. Since the transport dispersive model is well known for describing the mechanism underlying the peptides separation in a chromatographic column [13], numerical simulation will be performed to study the operating conditions, enabling peptides separation in IMAC.

Hence, in this review, we discuss first the various sources of MCPs and their production from proteins using enzymatic treatments. Indeed, MCPs can be separated from these complex mixtures of peptides, the so-called hydrolysates. Next, peptides-metal ion interactions are discussed to help understanding the mechanism inside an IMAC column. In a second part, IMAC is developed to understand the constituents and various steps of a typical IMAC separation process. Finally, the last part is dedicated to chromatography modelling using a transport dispersive model and simulation, where SPR data are used as input data for further separation simulation.

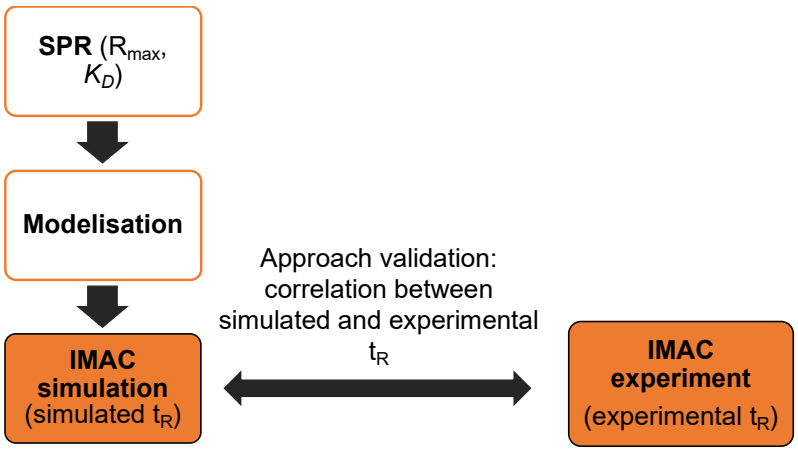

(**a**)

Figure 1. *Cont.*

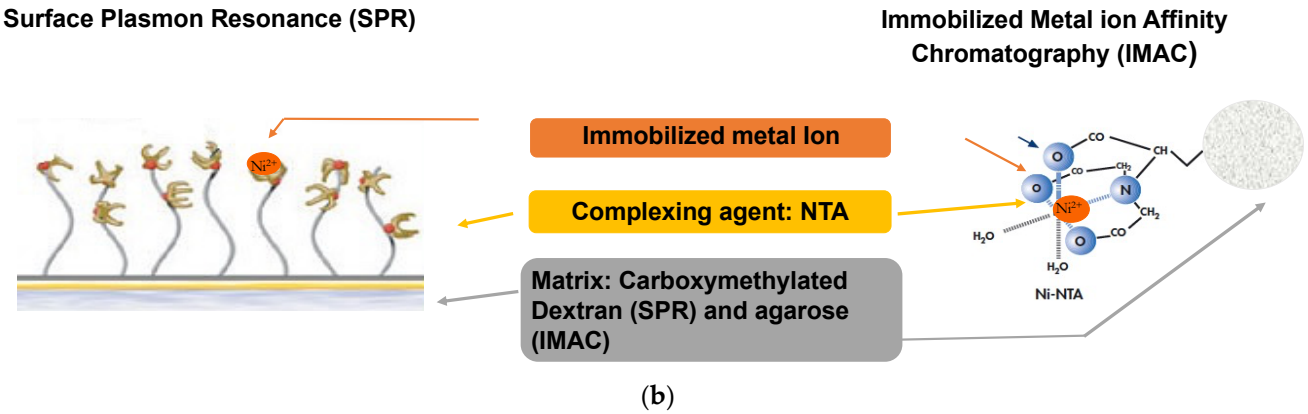

Figure 1. A simulation of Metal-Chelating peptides separation in IMAC (**a**) considering the analogy between IMAC and SPR (similar support, metal, complexing agent) (**b**). t_R retention time; R_{max} maximum Response; K_D Constant of dissociation.

2. Production and Applications of Metal-Chelating Peptides

This section is dedicated to various resources of Metal-Chelating Peptides and notably, how they are produced from protein using proteolysis. The last subsection focuses on the interactions between a metal ion and a peptide endowed with the metal-chelation properties, which are also at the basis of the MCPs separation in IMAC.

2.1. Metal-Chelating Peptides and Their Application

MCPs bind metals through the formation of peptide-metal ion complexes. Whatever the nature of metal ions, the ability of MCPs to complex them depends on several aspects [14], notably their N- and C-terminal groups, the nature of the side chains of the AA residues, and the accessibility of amide and carbonyl groups of polypeptide backbone. By complexing di- or trivalent metals (e.g., Ca^{2+}, Zn^{2+}, Fe^{3+} or Cu^{2+}), MCPs promote their better stability in solution, mineral absorption, and bioavailability [1,15–18].

MCPs present interesting applications focused on functional and nutraceutical product. Currently, the additives and functional applications of MCPs are mainly at the stage of laboratory scale [19], only few of them are commercialized [3].

MCPs can complex transition metal ions, such as Fe^{2+} and Cu^{2+}, involved in the reactive oxygen species (ROS) production via the Fenton and Haber Weiss reactions [19]. Indeed, these ROS can damage biomolecules and induce many degenerative, neurological, or cardiovascular diseases and even cancers [20–22]. Hence, MCPs can act as indirect antioxidant molecules [12,23,24], preventing oxidative damages and their related chronic diseases [25]. They also enhance the food shelf life, while reducing the toxic substances generated by oxidation phenomena, especially in meat [26].

MCPs can potentially be used as supplements in the treatment of diseases associated with mineral deficiency such as calcium, zinc and iron [17,27]. Furthermore, calcium-chelating peptides were applied in dairy-free functional food or beverage ingredients for lactose intolerant people, or for the prevention and treatment of osteoporosis [28].

Through metal complexation, MCPs can remove heavy metal (e.g., Cd^{2+}, Ni^{2+}, As^{3+}, or Pb^{2+}) from the environment [29], for decontamination applications for instance. MCPs can prevent corrosion by enhancing the biofilm adhesion on metal surfaces [30].

2.2. Various Protein Resources of Metal-Chelating Peptides

MCPs are reported in various food matrices from animal origin, e.g., Alaska Pollack backbone [31], beef muscle, chicken, cod, lamb, and pork [32], porcine blood plasma [33,34], egg yolk and white [35]. Furthermore, MCPs are found from aquatic sources such as oyster proteins [36], anchovy muscle proteins [37], and tilapia muscles [38]. Among all the animal proteins, milk proteins are the most famous ones for their MCPs content, either in

whole milk [39–41], bovine serum [42], or whey [43]. Indeed, Caseino-PhosphoPeptides (CPPs) increase solubility of metals such as zinc, calcium and iron in the intestine by the formation of metal-peptide complexes, enhancing their absorption and bioavailability [1]. Their mechanisms of action and bioavailability were investigated in vitro and in vivo [27].

MCPs were also reported from plant protein sources such as sunflower [44], sesame [15], soybean [45], wheat germen [46], barley [47], and mung bean [48] from Cucurbitaceae seeds [49]. Compared to plants, animal sources seem to be endowed with a higher nutritional and bioactive potential [15]. However, vegetal resources have recently arisen the interest from the scientific community, due to the environmental problems related to animal protein sources consumption [50].

In order to generate high added-value products, the use of protein-rich matrices from agro-industrial and co-products constitute the most interesting current topic on product development from food proteins [51]. Marine processing wastes and other agro-industrial by-products content a high percentage of protein (10–23% *w*/*w*) with high quality, thus becoming a potential source for bio-functional peptide production [28]. Calcium-binding peptides identified from tilapia scale protein were rich in aspartate and glutamate residues [52] such as the DGDDGEAGKIG peptide. Other by-products were also evaluated for their iron-chelating activities, including the Pacific cod skin [16], and Alaska pollock skin [53,54]. Recently, some studies [26,55] evaluated chicken by-products—notably skin and foot broth—as new and highly effective protein sources for obtaining iron- and calcium-chelating peptides, respectively.

Generally, metal-chelating activity exhibited by peptides is associated with the type and position of AA residues present within the peptide sequence [1,56]. Table 1 summarizes some peptide sequences identified from various food proteins and the corresponding chelated metal.

Table 1. Examples of metal-chelating peptides produced from different food protein sources, proteases used for hydrolysis and chelated metal.

Protein Source	Enzymes Used for Proteolysis	Metal-Chelating Activity	Peptide Sequence	Reference
Sesame	Papain, Alcalase, Trypsin	Zn^{2+} and Fe^{2+}	SM NCS	[15]
Alaska pollock skin	Trypsin, Flavourzyme	Fe^{2+}	SCH	[57]
Soybean	Protease M	Ca^{2+}	DEGEQPFPFP	[45]
Tilapia scales	Pepsin, Flavourzyme	Ca^{2+}	NGNNGEAGKIG	[52]
Antarctic krill	Trypsin	Ca^{2+}	VLGYIQIR	[58]
Oyster	Pepsin	Zn^{2+}	HLRQEEKEEVTV GSLK	[36]
Rapeseed	Alcalase	Zn^{2+}	AR NSM EPSH	[56]
Defatted walnut flake	Neutral protease	Fe^{3+}	LAGNPDDEFRPQ VEDELVAVV	[59]
Pacific cod skin gelatin	Trypsin, Alcalase, Flavourzyme	Fe^{2+}	GPAGPHGPPGKDGR AGPHGPPGKDGR	[53]
Scad (*Decapterus maruadsi*) by-products	Alcalase	Fe^{3+}	QKGTYDDYVEGL	[54]
Casein	Trypsin	Fe^{2+}	EDVPSER HKEMPFPK NMAINPSK	[39]
Peony seed	Alcalase	Fe^{2+}	AVPYPQR SMRKPPG	[60]

2.3. Proteolysis Production of Metal-Chelating Peptides

First, the protein is selected among a wide variety of sources. In a sustainable development strategy, current studies focused on protein sources from agro-industrial wastes [19]. Next, proteolysis is carried out, followed by separation, purification and identification of

target peptide. Sometimes, peptides are synthesized in order to validate their biological activities [1,19,61].

The proteolysis reaction breaks down proteins going from polypeptides to smallest peptides down to free AA residues. Naturally occurring in gastrointestinal digestion, hydrolysis can also be carried out using acids, temperature, various enzymes, microorganisms fermentation, or food processing, such as heat-and high-pressure treatment [2,62–64]. However, the enzymatic proteolysis is the most convenient and widely used method for MCPs production [2] since it is more controllable due to the stability, efficiency and specificity of the enzymes [65], while being safe, quick, and relatively inexpensive [25]. Upon proteolysis, MCPs are released through the effects of various proteases [56], whose properties depend on their specificity, proteolysis mechanism [66] and reaction advancement. Acid pre-hydrolysis treatments can lead to the protein degradation into high molecular mass polypeptides [49], thus facilitating the enzyme accessibility during proteolysis. The enzymatic action influences the structure, physicochemical and bioactive properties of degraded proteins [67].

Proteases are used either pure (e.g., pepsin, trypsin, papain, pancreatin, chymotrypsin, thermolysin, etc.) or under industrial complex mixtures (e.g., Neutrase®—bacterial proteases, Flavourzyme®—an aminopeptidase, Alcalase®—a serine endopeptidase, or Protamex®—a mixture of serine and metal endopeptidases) [3]. Enzymes are classified according to the broken bonds; endopeptidases (e.g., trypsin, chymotrypsin, pepsin, pancreatin, protease, actinidin, bromelain, papain, Alcalase®) act away from the N-/C-terminus, while exopeptidases (e.g., carboxypeptidase Y, aminopeptidase M, Flavourzyme®) break peptide bonds at the terminus of polypeptide chains [49]. Note that some enzymes are more specific in cleavage (composition of the cleavage site, pH) than others.

In addition to the enzyme specificity, other aspects must be taken into account [19], since the peptide functional and biological characteristics depend on the process conditions as well pH, temperature, time or the enzyme/substrate ratio [25]. Those former parameters affect the Degree of Hydrolysis (DH), characterizing the advancement of the proteolysis reaction. The calculated DH(%) represents the ratio of peptide bonds cleaved over the total protein peptide bonds [66,68]. According to the protein source and the proteolysis parameters, various peptide sequences can be obtained, endowed with various structural properties in terms of molecular size, hydrophobicity and AA composition [2].

The hydrolysis products include partially unhydrolyzed protein, polypeptides and free AA [19]. After proteolysis, MCPs must be processed based on their structural and physicochemical characteristics [51]. Membrane ultrafiltration, the first step before purification [61], can be carried out using various molecular weight cut-off membranes to concentrate the potentially bioactive fraction. Next, IMAC, gel filtration chromatography, ion exchange chromatography and reverse phase high performance liquid chromatography are used for hydrolysate purification and MCPs obtention [1]. Finally, the isolated MCPs are identified by mass spectrometry, using either electrospray ionization (ESI) by a coupling LC-ESI-MS, or matrix-assisted laser desorption ionization time-of-flight (MALDI-TOF), commonly used due to their high sensitivity and low detection limit [19]

2.4. Peptides-Metal Ion Interactions

2.4.1. The Hard and Soft Acid and Base Theory

The elucidation of peptides-metal ions interactions is mainly based on the hard and soft acids and bases (HSAB) theory. This theory states that in order to form a bond between two atoms, one atom behaves similar to a Lewis acid while the other one behaves similar to a Lewis base [69]. Metal ions are electron pair acceptors, and thus are Lewis acids, while peptides are electron pair donors, and thus are Lewis bases.

The bond strength depends on the ratings of hardness/softness of two atoms involved in the interaction, the hard base-hard acid bonds or soft base-soft acid bonds being the strongest; hard-soft interactions result in relatively weak complexes [5,70,71]. In peptide-metal ion interactions, this theory predicts which metal ions and AA can interact most

favorably. Table 2 reports some examples of the classification of metals and AA residue, according to Pearson and co-workers [70]. The HSAB classification is based on different properties such as charge density, polarizability, electronegativity, and energy of orbitals involved, which determine the covalent or ionic nature of peptide-metal interactions.

Table 2. HSAB theory adapted from Pearson and co-workers.

	Hard	**Borderline**	**Soft**
Properties	High charge density, hardly polarizable, prefer ionic interaction	Intermediate	Low charge density, polarizable, prefer covalent interactions
Acids	H^+, Li^+, Na^+, K^+, Be^{2+}, Mg^{2+}, Ca^{2+}, Sr^{2+}, Sn^{2+}, Cr^{3+}, Co^{3+}, Fe^{3+}, As^{3+}, Ir^{3+}, Al^{3+}, Sc^{3+}, Ga^{3+}, In^{3+}, La^{3+}, Si^{4+}, Ti^{4+}, Zr^{4+}, Th^{4+}, Pu^{4+}	Fe^{2+}, Co^{2+}, Ni^{2+}, Cu^{2+}, Zn^{2+}, Pb^{2+}, Mn^{2+}	Cu^+, Ag^+, Au^+, Ti^+, Hg^+, Cs^+, Pd^{2+}, Cd^{2+}, Pt^{2+}, Hg^{2+}
Bases	Carboxylate group (aspartic and glutamic acid), hydroxyl group (serine, threonine, tyrosine), phosphorylated amino acids	Aromatic nitrogen (histidine, tryptophan), amides (asparagine, glutamine), aliphatic nitrogen	Cyanides, sulphur groups (cysteine, methionine)

2.4.2. Effect of Various Parameters on Peptide-Metal Ion Interactions

Various parameters can affect the peptide-metal ion interactions notably the position and number of active residues. The coordination behavior depends mainly on the position of effective donor atoms of the side chains within a peptide sequence and also on the type of the metal ion involved in the interaction. For example, the amino group of the N-terminal residue and various highly coordinated side chain residues (thiol, phosphonic and imidazole residues) at the appropriate locations serve as an anchor for binding metal ions in solution, preventing metal ion hydrolysis. His in the 3rd position provides an extra stability to metal complexes with Cu^{2+} and Ni^{2+} through the metal ion-promoted amide backbone deprotonation and coordination in free solution [72,73]. In polyhistidine-containing peptides (such as His6-tag), His sequential proximity favors the complex formation [74,75], but the influence of spatial separation of histidine is metal ion dependent. In this case, the metal ion has a multiplicity of imidazole nitrogen atoms to bind, thus a variety of coordination modes and structures are possible.

Furthermore, the charge of the residue side group can also affect the interactions between a peptide and metal-ion; thus, for side chain group positively charged such as in lysine or in arginine even in basic solution, the complex is less stable (or not formed) due to repulsion phenomenon [76]. Negatively charged side chain group such as glutamate and aspartate, attract the positive charge of metal ion (opposite charges attraction) and form strong and stable complexes [5].

The pH of environment can also affect the peptide-metal ion interactions since proteins and peptides are electron pair donors not only for metal ions but also for protons. Hence, competition between metal ion and proton may occurs, explaining that the stability of a complex depends on pH. A decrease of pH leads to the decrease in binding coefficient as H^+ displaces the metal ions by protonating the coordinated $-S^-$, $-NH_2$, $-COO^-$, imidazole or amide groups [5]. A molecular dynamic simulation can enable to study interaction between peptide and metal ion, however, it is out of the scope of this review.

3. Immobilized Metal Ion Affinity Chromatography for Metal-Chelating Peptides Separation

Once hydrolysates are produced from proteins, MCPs can be separated from these complex mixtures of peptides using IMAC, a technique based on peptide-metal ion interactions.

3.1. Generalities on IMAC

In 1974, a new technique of affinity chromatography was developed and used for metalloproteins separation [77]. The IMAC—introduced in 1975 as a metal chelate chromatography by Porath—was then used for the fractionation and purification of proteins containing histidine and cysteine residues [78]. While the separation of nucleotides was the initial objective of IMAC, other applications were evidenced for antibodies, enzymes and recombinant proteins immobilization, for instance [79].

IMAC is mainly based on the interactions between the immobilized metal ion and the electron donor groups of molecules that flow in a mobile phase [79–81]. These interactions depend on the nature of IMAC constituents (i.e., matrix, complexing agent and immobilized metal ion), but are also affected by the physicochemical conditions inside the column.

IMAC has three main parts [82]: the matrix (e.g., cellulose, silica, agarose) fixed via spacer arms to the chelating agents (e.g., iminodiacetic acid (IDA), nitrilotriacetic acid (NTA)), onto which are immobilized the metal ions (e.g., Ni^{2+}, Cu^{2+}, Fe^{2+}, Co^{2+}). Each specific constituent of the IMAC chromatographic phase is detailed hereafter.

3.2. The Constituents of IMAC Chromatographic Phase

3.2.1. The Matrix

The matrix (or resin) is the stationary phase on which metal ions are fixed via a complexing agent and a spacer arm. Either organic or non-organic, the matrix impacts the stability of the complex formed between a metal ion and a proteinous molecule (e.g., peptide or proteins) [5]. Between the matrix and the chelating agent, a short alkyl chain (the so-called spacer arm) is grafted to ensure accessibility. The IMAC column can be purchased already filled with the matrix grafted with the complexing agent [59,83–85] or the matrix can be bought separately [86–90]. Inversely, an initially empty column can be filled with resins [15,57,91,92].

A good matrix is easily activated, highly hydrophilic and characterized by low non-specific adsorption, and has a high porosity to fix a large number of ligands [82]. Furthermore, it requires a good chemical, physical and mechanical stability for high flow rates and to avoid its denaturation due to eluent incompatibility [82].

Two types of matrices exist, depending on the nature of the phase. For capillary phases, the adsorption occurs on their surface; however, a high-pressure drop is observed which does not long resist to strong mechanical forces (e.g., agarose) [6]. In comparison, for porous phases, the adsorption takes place inside pores, thus increasing the number of molecules able to be fixed. Furthermore, some non-porous gels were developed such as microspheres either made of fused silica [93] or styrene-divinylbenzene [86].

The common matrices used to separate peptides/proteins are agarose-based, generally grafted with IDA [93]. Other matrices were developed using cellulose [94], chitin [92], fused silica [95] or synthetic polymers [96]. Nevertheless, to the author's knowledge, other matrices based on carbon and graphene were not reported to date for IMAC applications.

3.2.2. Complexing Agents

In IMAC, complexing or chelating agents immobilize the metal ions by complex formation. Each agent is characterized by a coordination number/denticity, a specific charge, steric bulk and chirality [82], which directly influence the binding of metal ions-molecules of interest. According to the coordination geometry, the complex agent is characterized as monodentate, bidentate, and so on [6,97]. Four types of complexing agents were principally investigated, depending on their denticity (Figure 2): bidentate (e.g., aminohydroxamic acid, salicylaldehyde, 8-hydroxyquinoline (8-HQ)), tridentate (e.g., IDA [93], dipicolylamine (DPA), ortho-phosphoserine (OPS), N-(2-pyridylmethyl)aminoacetate, 2,6-diamino methylpyridine), tetradentate (e.g., NTA [79,98], carboxymethylated aspartic acid (CM-Asp) [99] or pentadentate (e.g., N,N,N′-tris(carboxymethyl) ethylene diamine (TED) [100].

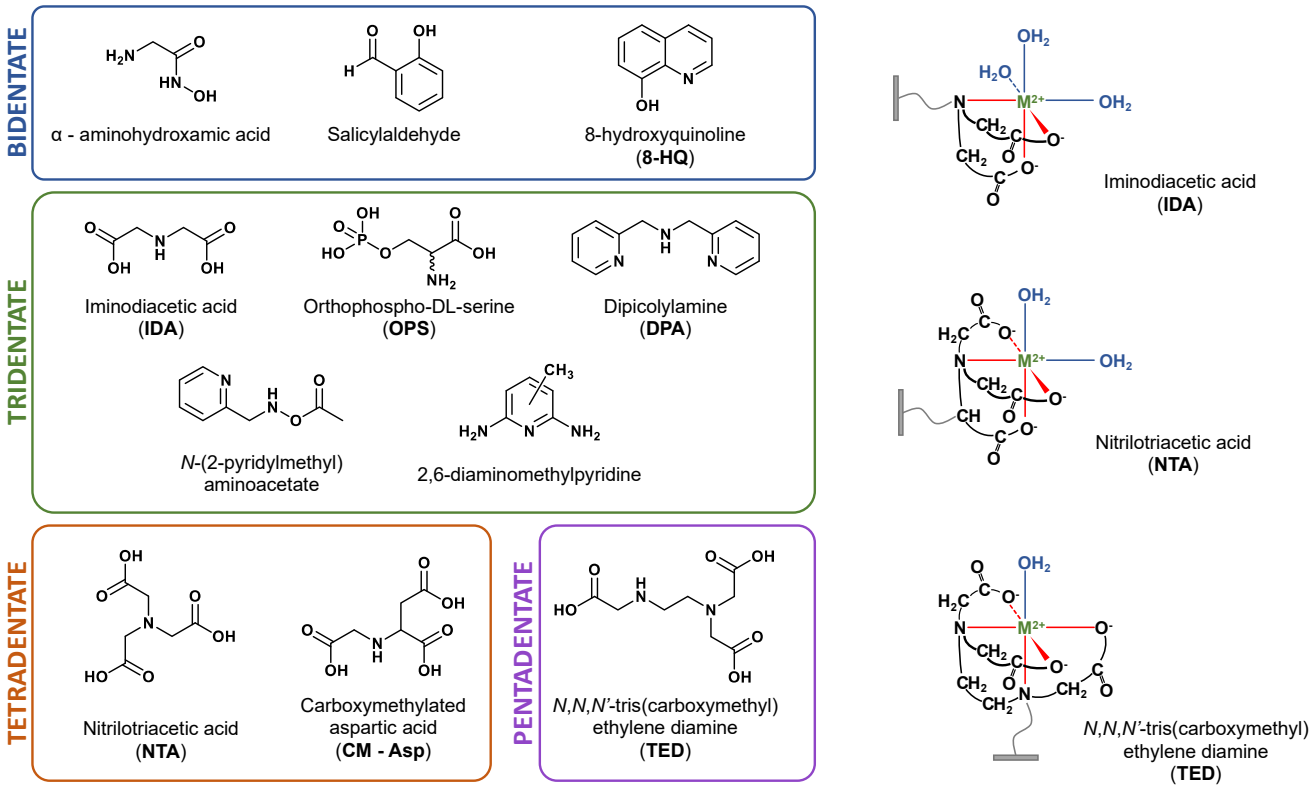

Figure 2. Different complexing agent used in IMAC and representation of the spatial organization of the ligand around the metal ion.

When a complexing agent has a high denticity, it bonds the metal ion with a high coordination number, and thus, the selectivity towards the ligands of interest increases because the number of free sites remaining on the metal center to bind peptides/proteins is limited. Therefore, tri- or tetradentate complexing agents are preferentially used. Indeed, there is a strong metal ion immobilization with multidentate chelating agent. However, the stronger the metal- chelating agent interaction, the lower the metal ion leakage from the support, but also the lower the number of free remaining sites to bind the targeted ligands [69,82,89,101].

The NTA, IDA and TED are the most commonly used complexing agents [97] with a good compromise. Note that the NTA purification of recombinant proteinous molecules leads to a better purity compared to IDA, due to a higher metal ion leakage in this latter case [102,103].

3.2.3. Immobilized Metal Ions

To target a specific class of residues, present in peptide/protein mixtures, the HSAB theory can guide the choice of metal ion immobilized on the IMAC column. However, this HSAB theory is not always appropriate and rather give a general trend [15,88]. For example, Cu^{2+} can bind a proteinaceous molecule with only one exposed histidine residue, while Ni^{2+} and Zn^{2+} need two exposed vicinal histidine residues, and Co^{2+} requires at least two adjacent exposed histidine residues to bind protein/peptide [81].

In some cases, the metal ion is selected and immobilized without focusing on a particular AA residue present in peptides [16,53,57]. Furthermore, metal ions can be selected according to the final application. For instance, tri- and tetravalent ions (Fe^{3+}, Ti^{4+}) are preferred for phosphoproteins purification while divalent Ni^{2+} ions are used for histidine-tagged proteins purification due to their redox stability and intermediate polarizability [69,82].

3.3. The Various Steps of IMAC Separation

3.3.1. General Principle

IMAC is based on the affinity of each targeted peptide/protein with metal ions immobilized on the matrix [79,81,82,104], and interactions that occur between a peptide and a metal ion are developed in Section 2.4. Globally, biomolecules are first adsorbed and then desorbed (elution) [97]. IMAC comprises these main steps: column equilibration with buffer solutions, sample loading followed by washing to remove the unbound components, elution of bound components, column stripping and regeneration with the metal (Figure 3).

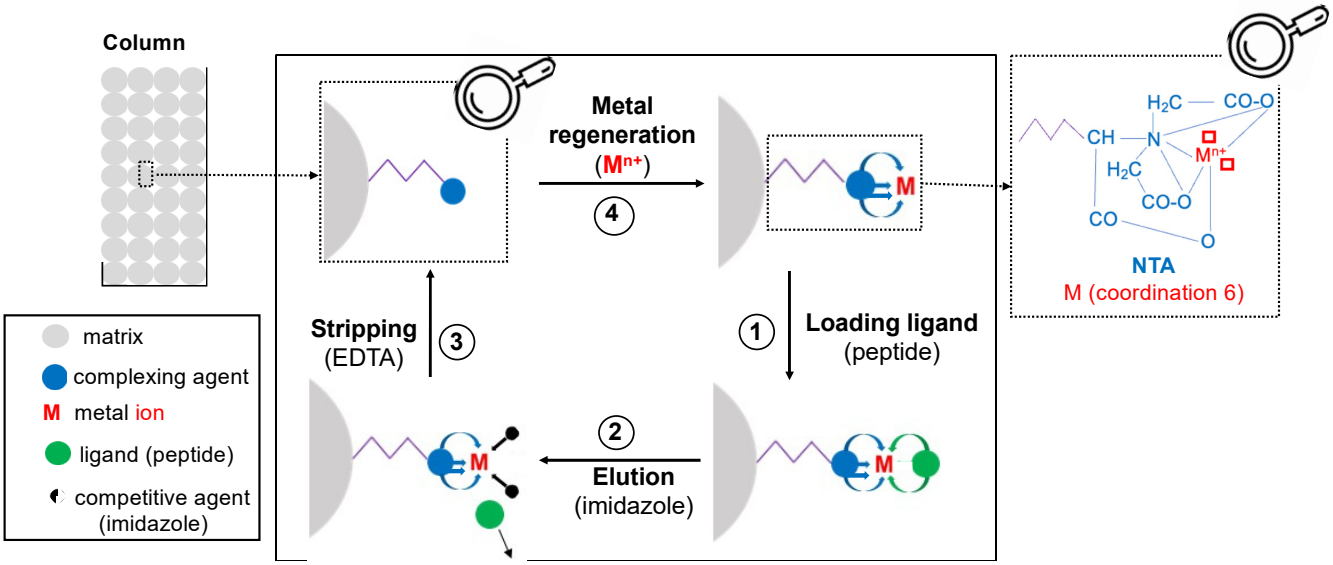

Figure 3. The Main steps involved in immobilized metal ion affinity chromatography: 1. Loading the ligand; 2. Elution of the ligand; 3. Stripping of the metal on column; 4. Metal regeneration on the column (figure adapted from thesis manuscript [105]).

3.3.2. Metal Ion Loading and Equilibration of the Column with Buffer Solutions

Metal ions are frequently loaded onto resins in their hydrochloride form [106–108] or as sulfates salts [15,90,91]. The metal ions loaded in excess are removed using either sodium chloride solutions, a weak complex agent such as acetate [59,109], a low concentration of a strong complexing agent (phosphate, <50 mM) [110,111], or simply with deionized water. Next, the column is equilibrated with the loading buffer (i.e., the buffer used to dilute the samples).

3.3.3. Sample Load and Injection

The loading buffers commonly used in IMAC are non-volatile and based on phosphates (i.e., monosodium, disodium, trisodium) or zwitterionic sulfonated molecules (i.e., MES, HEPES and MOPS), which minimizes the interactions with the complexing agent [112]. Sodium chloride (NaCl, 0.1–3 M) is generally added to reduce the non-specific interactions [99].

When phosphopeptides are investigated, acetic acid can be used as a loading buffer [113] due to the low pK value of phosphate group; organic solvent such as formic acid/acetonitrile [86], methanol/acetonitrile/acetic acid [85] or trifluoroacetic acid [114] or non-organic acid such as hydrochloric acid/potassium hydrogen phthalate [91] are also reported.

3.3.4. Removing the Unbound Components

Unbound components are removed using the loading buffer or deionized water [15,88,90–92,106,113]. When water is used for washing, it is followed by a second wash with a weak complexing agent such as formate or acetate [45,59,94,109,115]. In other works, formic or acetic acids were used for washing [86] to remove impurities.

3.3.5. Elution of Targeted Compounds

The targeted proteins/peptides are eluted from the column in three various ways: either acting on the pH, using a competitor agent, or by destructing the chelates [6,79], as described hereafter (Figure 4).

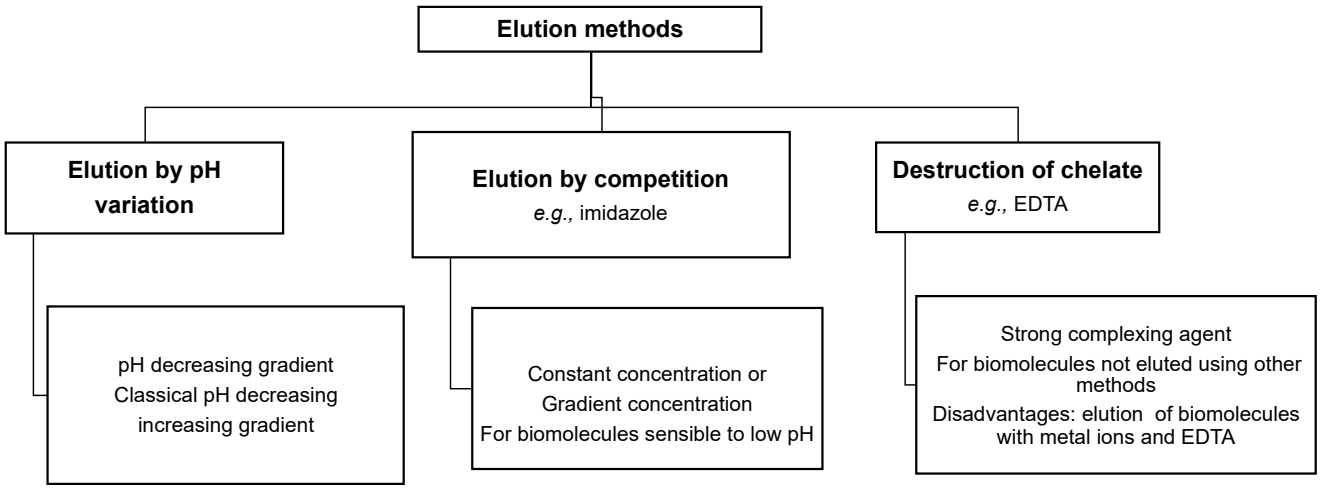

Figure 4. The elution methods commonly used in immobilized metal ion affinity chromatography.

Decreasing the pH can be used to elute peptides, since the bound groups such as imidazole are protonated upon acidification. The protonation induces the breaking of the coordination bond, thus leading to the proteins/peptides removal [16,53,89,110,111,116–119]. Sometimes, elution cannot be carried out by decreasing the pH (case of human immunoglobulin (IgG) on Co^{2+}) [119], since some molecules are unstable at low pH, and other alternatives such as competitive displacement must be considered. For metals classified as hard acids such as Fe^{3+}, elution can be carried out by increasing the pH gradient, corresponding to a competition with OH- ions. Chaga et al. [81] purified amyloglucosidase on Fe^{3+}-IDA-agarose, first by increasing the pH and then by using a sodium phosphate solution.

Furthermore, competitive displacement (the so-called ligand exchange) is specially used for molecules sensitive to low pH. The eluent used is a competitive agent (e.g., imidazole) with a higher affinity for the immobilized metal ion than the biomolecules to be eluted. This eluent is introduced into the chromatographic column, leading thus to the ligand exchange. According to the type of peptides, the competitors used can differ. For metals classified as hard acids such as Fe^{3+}, elution can also be carried out by adding competitors such as organic acids (e.g., acetonitrile) and phosphates in the mobile phase. For non-phosphorylated peptides, histidine residues are more frequent and accessible for interactions [116,120]. Thus, elution is carried out by a competitive displacement using imidazole applied in isocratic [121,122] or in gradient modes [96,99,117,123] in order to elute histidine-containing peptides. When the carboxylate is the donor group of the ligands to elute, the competitors are generally phosphate groups used either at constant concentration [45,115] or with a gradient [45]. For the phosphorylated peptides, the phosphate is the donor group of interest. Hence, hydroxide ions (OH^-) are also used as competitors [91,113], either in isocratic mode or in gradient mode [86,106], which consequently induces a pH increase. Competition by other phosphates groups [107,108], or other groups such as ascorbate [85] or trifluoroacetate [114] can also be used at constant concentration (isocratic mode).

In addition, very strong complexing agents such as EDTA can be used for peptides elution by breaking bonds between metals and the complex agent on which metals are immobilized. Indeed, the metal ion-EDTA complexes are eluted in the meantime than the peptides, thus an additional separation process is required [101]. This latter method is only used when all other methods are not effective. In the particular case of the selenoprotein P,

its interaction with Cu^{2+} immobilized on IMAC was so strong that the protein-metal ion complex could only be eluted by EDTA [124].

3.3.6. Column Stripping

After each assay, the column is usually washed using a strong complexing agent (EDTA, 10 to 50 mM) to remove the remaining immobilized metal ions [88,110,115,125]. Salts such as sodium chloride and sodium hydroxide solutions are sometimes additionally used as solutions for cleaning up all impurities.

3.4. Parameters Affecting IMAC

3.4.1. Generalities

The IMAC separation of molecules is mainly based on the interactions between metal ions and AA residues of peptides/proteins. However, other factors can also influence this process such as the type of metal ion immobilized onto IMAC, the chelate structure, the adsorbent nature, the protein structure and the environment. This section focuses on the effects related to the surrounding environment (e.g., pH, type of buffer, ionic strengths, salts, temperature, detergents used, presence of alcohols) [101].

3.4.2. The pH of the Environment

This important parameter must be taken into account in IMAC experiments because it has a high impact in retention and elution of proteinaceous molecules [126]. Indeed, the pH affects the nucleophilic behavior of the buffer components, the electron donor /acceptor properties of the solutes and the metal stability [5]. At pH lower than the isoelectric point (pI) of proteinaceous molecules, these molecules are positively charged and can bind to the negatively charged complexing agents such as NTA and IDA. This could be interesting in loading phase for the purpose of optimizing the binding of molecules onto immobilized metal ion.

3.4.3. The Salts

Salts such as sodium chloride are often added into buffers to minimize the ionic interactions occurring between the proteins and the resin but also between proteins themselves. The sodium chloride concentration used varies according to the authors in the ranges 0.1–1 M [6,79,82,97] and also on the biomolecules investigated. Pavan and colleagues [99] did not improve the separation of human IgG in serum using NaCl solution and IMAC charged with Ni^{2+} and Co^{2+} immobilized onto carboxymethylaspartate, grafted onto a poly (ethylenevinyl alcohol) matrix. According to former authors, the addition of NaCl in loading buffers, which acts on the ionic strength of the solution, probably modified the pKa of coordinating groups on proteins and increased hydrophobic interactions, thus decreasing IgG binding on Ni^{2+} and Co^{2+}.

Salts can also weaken the force between water and immobilized metal ion and consequently facilitate the adsorption of protein [126]. Decreasing salt concentration can thus lead to some protein desorption [5]. Sometimes, the competition between proteins and salts for the immobilized metal ions can also be a problem [126], especially for ammonium hydroxide (NH_4OH) or ammonium chloride (NH_4Cl). The presence of ammonia NH_3 in solution, in equilibrium with NH_4OH or NH_4Cl, can disturb the separation by its competitive effect for the metal sites [15]. Increasing the ionic strength of buffer by adding salts can eliminate undesirable unspecific interactions and enhance selectivity, thus the binding of protein/peptide increases by promoting purely complexing interactions between ligands and metal ions.

3.4.4. The Organic Solvents and Detergents

Hydrophobic interactions can also occur between the ligands (protein/peptide) and the support [99,127]. To minimize these undesirable interactions, organic modifiers such as

glycerol (up to 50% v/v), ethanol (up to 20% v/v) [6], or acetonitrile (ratio 1:1 (v/v)) [114] can be added to the loading buffer.

Furthermore, detergents such as Tween 80® (0.01% v/v) or 1% Triton X-100 [6] are sometimes used in IMAC to enhance selectivity and minimize unspecific interactions.

Finally, other chemicals, notably reducing agent such as β-mercaptoethanol can be added to improve the separation [6] while reducing the formation of disulfide bridges.

3.5. Application of IMAC for Metal-Chelating Peptides Separation

3.5.1. Metal-Chelating Peptides Separation and Purification in Hydrolysate

IMAC, mostly used for the enrichment and purification of MCPs or proteins, is routinely considered as one of the first stage in their purification [1]. The few examples reported in this section focuses on metal ions, known as intermediate Lewis acids. In order to bind immobilized metal ions such as Ni^{2+}, the complementary ligand must contain histidine (H), cysteine (C) or tryptophan (W) residues [6].

Guo and co-workers [16] used IMAC charged with various metal ions for the MCPs purification from Alaska pollock skin collagen hydrolysates. Various chromatographic profiles of peptides were obtained onto each M^{2+}-IMAC column, indicating that the nature of MCPs separated was different as a function of the targeted metal ion. Wang and colleagues [15] applied IMAC for the purification of Zn^{2+}-chelating peptides from sesame protein hydrolysate. Likewise, MCPs were purified from the oyster protein hydrolysate [36] and rapeseed protein hydrolysate [56], respectively.

3.5.2. Separation and Purification of Recombinant Proteins/Peptides

The addition of a short tail of histidine residues on N- or C-terminal of a peptide/protein can improve its separation and purification in IMAC. The most often used histidine tag is comprised of six consecutives histidine residues [69,102,128]. After purification, histidine tags are often removed, notably for pharmaceutical applications [69].

The separation can also be carried out when a peptide mixture contains both non-metal chelating and metal-chelating peptides. For example, the recombinant Luteinizing Hormone-Releasing Hormone (LHRH) analog 2–10 LHRH, which contains chelating peptides with His-Trp residues, shows an affinity with Ni^{2+}. On the contrary, the 3–10 LHRH and the 4–10 LHRH do not present metal-chelating properties and thus, cannot interact with Ni^{2+}. Hence, the 2–10 LHRH can be separated from the LHRH mixture using Ni^{2+} in IMAC [104]. The Cu^{2+}-NTA or Ni^{2+}-NTA is the most common combination used for efficient and selective purification of metal-chelating molecules [129].

3.5.3. Adsorption and Concentration of Histidine-Containing Peptides

Histidine-containing dipeptides such as carnosine (β-alanyl-L-histidine) and anserine (β-alanyl-L-1-methylhistidine) are widely used in pharmaceutical and food industries. Indeed, these antioxidants are metal-chelators notably used as food additives and in the treatment of Alzheimer's diseases [130] such as other MCPs [60,131,132]. Oshima and co-workers [133] studied their separation and concentration from a saline solution using the Cu^{2+}-IDA-IMAC.

4. Simulation of Metal-Chelating Peptides Separation from Surface Plasmon Resonance Experimental Data

Separation processes can be expensive and time consuming, therefore simulation can be used to predict peptides separation before launching expensive experiments. This section discusses isotherm determination by SPR, which are used as input data in chromatography modelling using a transport dispersive model for further peptide separation simulation.

4.1. Peptides Investigated for Simulation

Peptides sequences used to build a model for MCPs separation simulation can be selected from the literature or designed manually or using a software. For peptides reported

from the literature, their ability to chelate a given metal have been previously studied. Hence, they can be used as a positive or negative reference. For designed peptides, peptide-metal ion interactions are expected according to the HSAB theory (see Section 2.4.1). In this case, the number and position of the target AA residues in the peptide sequences are important parameters to consider [23].

After identifying the peptides to study, the corresponding sequences are chemically *synthetized* [134,135] by several chemical manufacturers (e.g., GeneCust (Boynes, France), PolypPeptides (Zug, Switzerland), Alberta Peptide Institute (Edmonton, Alberta, Canada). Synthesis can be carried out either by Liquid Phase Peptide Synthesis (LPPS) or Solid Phase Peptide Synthesis (SPPS). SPPS—developed for the first time by Merrifield [136]—is the cheapest, the fastest, the most efficient and the most popular technique for the production of synthetic peptides [137].

For validating the model, IMAC separation can be then performed on synthetic hydrolysates produced by mixing synthetic peptides. Knowing the mixture composition, it facilitates the behavior's study of each peptide present in synthetic hydrolysate. Finally, real protein hydrolysates can also be investigated to ensure that the model works perfectly.

4.2. Affinity Constant Determination Using Surface Plasmon Resonance

4.2.1. Surface Plasmon Resonance Principle

SPR, an optical biosensor, which quantifies the interactions between various biomolecules (e.g., peptides, proteins, etc.) [138], is used to investigate the molecular adsorption and the change of surface structure at a nanometric scale [139]. It is commonly used to evaluate kinetics and thermodynamics of interactions between two biomolecules [140–142]. SPR is also used in pharmaceutical analysis and food analyses, medical diagnostic and environmental monitoring [143], and this section discusses the benefits of SPR on MCPs applications.

In SPR terminology, and for MCPs investigation, the metal is immobilized onto the sensorship surface using covalent or non-covalent bonds according to its nature [138]. Metal ion is fixed by a chelating agent (NTA), which is covalently attached to the monolayer of carboxymethylated dextran on the golden surface of the sensorship. Ni^{2+}-NTA surface is frequently used for immobilization applications as it reduces the leaking of immobilized molecules [128,144,145], and provides a high sensitivity. However, the sensing surface can become unstable notably due to the progressive dissociation of the bound biomolecule, the use of low pH, complex matrices, the injection of reducing agents and chelators (e.g., imidazole, EDTA), competing with imidazole group of histidine residues present in protein or peptides. More stable interactions could be obtained by using multivalent surfaces (e.g., bis-NTA, tris-NTA), which increase the affinity for histidine tags such as 6His [146]. Other types of immobilizations exist in SPR but are out of the scope of this review.

After the metal ion immobilization, the peptide analyte is injected. Circulating over the sensor ship surface, it interacts or not with the immobilized molecule. When an interaction does occur between the Ni^{2+} and the peptide, the polarized light, which strikes the golden surface of the sensorship, is reflected to a certain angle. The affinity of the flowing peptide for the immobilized metal ion induces a change in refractive index (RI) of the polarized light, i.e., a change of the angle; this is the so-called plasmon angle [141,147–152]. The recording of the plasmon angle variation produces a sensorgram, i.e., a plot of the binding response expressed in resonance units (RU) as a function of time. For each studied concentration, the resonance is recorded at equilibrium point and plotted as a function of the analyte concentration in order to obtain a sorption isotherm. This latter can be fitted by various mathematical models (such as 1:1 metal: ligand binding model) to determine the dissociation constant (K_D). This one is expressed in M for pure synthetic or in M equivalent glycine for hydrolysate (complex mixture of peptide); in this latter case, a peptide quantification present in hydrolysate is required by OPA dosage [12].

Before studying another concentration, the sensing surface is regenerated using either competitive agents (e.g., EDTA) [12,153] or by decreasing the pH [154], or combining both

previous methods or adding detergents such as SDS [143]. The molecule to immobilize is then injected for the future cycle.

4.2.2. Affinity Constant Determination of Metal-Chelating Peptide for an Immobilized Metal Ion

The affinity constant (K_A, M^{-1}) is the inverse value of the apparent equilibrium dissociation constant (K_D, M), determined using mathematical adjustment such as the 1:1 binding model [128,155]. This 1:1 binding model connects the resonance response during steady state phase R (RU), the analyte concentration C (M) and the saturation response R_{max} (RU) via the Equation (1):

$$R = \frac{R_{max}C}{K_D + C} \quad (1)$$

K_D is obtained by a mathematical adjustment of former Equation (1) and is defined according to the Equation (2) of equilibrium:

$$PM \rightleftharpoons P + M, \text{ where } K_D = \frac{[P][M]}{[PM]} \quad (2)$$

where: [*P*] is the molar concentration of the peptide or protein, *[M]* is the molar concentration of the metal ion, and *[PM]* is the molar concentration of the complex formed [120].

In the K_D definition, charges are ignored for simplicity. Hence, K_D rarely expresses what really happens in the reaction since the stoichiometry of species—which is not always 1—also depends on the initial concentrations of peptide/protein, metal ion and their respective ratio. Therefore, different geometry of complexes can be formed on the same binding site for various experimental conditions; thus, K_D measured at equilibrium highly depends on experimental conditions, which renders difficult the comparison with other studies [156].

Various studies on peptide-metal ion interactions used SPR successfully. For example, MCPs present in various protein hydrolysates were quickly screened by Canabady-Rochelle and colleagues [12] leading to a fast determination of the peptide-metal ion affinity constants, subsequently correlated with their chelation capacity, determined in UV spectrophotometry. In this latter case, K_D was expressed in M equivalent glycine after OPA quantification. In addition to the affinity constant determination, the SPR angle shift also gives the association and dissociation kinetic constants (k_{on}, k_{off}) between two molecules [145,157], and were previously applied in the case of peptide and metal ions [47]. The volume of biomolecules per unit area, the conformational folding can also be obtained by SPR [139,140,147].

The SPR has a high sensibility for the interactions investigated since the K_D measures range from millimolar to nanomolar level; in addition, it gives a fast response [158] and uses small quantity of samples [140,159]. According to the Biacore® chip specification (product code: BR100407, cytiva (Massachusetts, USA)) and considering the chip thickness, a response of 100 RU represents a protein concentration of 1 g/L. Therefore, a value noted q_{max}, SPR can be calculated with the Equation (3):

$$q_{max,SPR} = \frac{R_{max}}{100} \quad (3)$$

where q_{max} is the liquid phase concentration of peptide/protein at the NTA sensor chip interface (g/L), and R_{max} is the maximal resonance (RU).

4.2.3. Analogy between IMAC and SPR

Both IMAC and SPR are based on peptide-metal ion interaction mechanisms (Figure 1a). Metal ion (e.g., Ni^{2+}) is immobilized by a complexing agent (e.g., NTA, IDA, TED), and the analyte (peptide or protein) exhibiting metal-chelating properties and circulating in the solution, binds more or less strongly to the metal ion depending on the affinity. Whatever the

technology, the metal ion is immobilized onto a complexing agent, and regeneration can be carried out in the same way.

When all accessible metal ion-binding sites are occupied by the peptides analyte, Rmax is determined in SPR while qmax is obtained in IMAC when the whole surface of the stationary phase is occupied by the analytes [160]. For both technologies, the working steps are the same. First, the metal ion is loaded using metal salt (e.g., $NiSO_4$) in the IMAC column or on the SPR chip. Secondly, the sample is loaded with the same phosphate buffer at pH 7.4; note that 0.005% of Tween 20 is added in SPR in order to protect the microfluidic chip. Next, elution is done in both technologies using a solution of imidazole (constant concentration in SPR; gradient concentration in IMAC). Finally, the support is regenerated using competitive agent such as EDTA in both technologies. For SPR, Rmax and K_D (and hence, K_A) parameters are obtained from SPR sorption isotherm while a retention time (t_R) is obtained in IMAC in the case of peptide injection. In the case of imidazole elution, this t_R value can be expressed in IMC which corresponds to the imidazole concentration used to elute the peptide. A low K_D or a high t_R (high IMC) corresponds to high affinity of a given peptide for the immobilized metal ion.

SPR and IMAC are complementary technologies which enable to study interactions between immobilized metal ions and peptides, thus SPR data can be used to further simulate IMAC separation. Analogies and differences between SPR and IMAC are summarized in Table 3.

Table 3. The analogy between SPR and IMAC.

	IMAC	**SPR**
Constituents	Same metal ion immobilized (e.g., Ni^{2+}) Same complexing agent (e.g., NTA) Matrix to support the complexing agent (e.g., agarose)	Matrix present too (e.g., carboxymethylated dextrane)
Experimental steps	Sample loading using a phosphate buffer at pH 7.4	Same sample loading added with Tween 20 for microfluidic
	Elution by competition (imidazole; isocratic or gradient mode)	Elution by competition (imidazole, isocratic mode only)
	EDTA Striping and metal ion regeneration (e.g., $NiSO_4$)	
	Flow rate: 1 mL/min for 1 mL bed volume	Flow rate: (20 µL/min)
Main results	Sorption isotherm used to illustrate the interaction between the metal ion and the biomolecules	
	Time of retention (t_R) of peptide	Dissociation constant (K_D)
	IMC: Imidazole concentration enabling elution	R_{max}
Advantages and disadvantages	Use of high volumes of buffers (~mL) Peptides separation	Use of small volumes for buffers (~µL) Peptide screening

4.3. Simulation of Chromatographic Separation

4.3.1. Principle

Phenomena occurring inside chromatographic columns can be modelled using mathematical equations. The optimum modeling and simulation require an understanding of mechanisms governing the processes such as equilibria (thermodynamics), hydrodynamics and kinetics. These models, based on the physicochemical mechanism underlying the process, are efficient compared to empirical models and are used as predictive tools before passing on experiments step [161]. Once established, numerical simulation can be carried out to observe the influence of various parameters on the separation efficiency thus, reducing the costs and the number of experiments to perform. Among these parameters, there are the concentration and volume of the sample loaded [162], the concentration and composition of the mobile phase (elution buffer), the particle diameter of the stationary phase, the column dimensions and porosity, the flow rate, axial dispersion coefficient, equilibrium isotherm, and mass transfer coefficient [163]. However, difficulties are often

observed in numerical resolutions of equations and it is necessary to make some hypothesis and assumptions for simplification while remaining realistic [164].

Generally, two approaches are used to model a chromatographic column and applied for IMAC column: first, the axially dispersed plug flow model and secondly, the stirred tank reactor cascade model. Both can be used to determine the so-called IMC (i.e., the imidazole concentration needed to elute the bound peptides), a parameter related to the retention time (t_R) of the MCPs in the column [165].

Other types of peptide separation were modelled based on their physicochemical properties (e.g., hydrophilicity); they were combined either with linear or multilinear regression [166–174], or using nonlinear approaches such as least-squares support vector machine and Gaussian process [123] or kernel function [175]. Finally, artificial neural networks [176] were studied, but only few are based on process mechanism such as axially dispersed plug flow model [135,160].

4.3.2. Adsorption Modeling

Adsorption is defined as the fixation of molecules or ions from a solution (mobile phase) to the solid surface (stationary phase). It is characterized by the equilibrium relationship between the concentration C_i of a compound i in the mobile phase, and its concentration qi in the stationary phase at a given temperature. This equilibrium relationship can be described by various adsorption isotherm models as stated later. The understanding of adsorption isotherm is essential since some of its parameters are used as input data for chromatography modelling and simulation. However, the choice of adsorption isotherm model can be hard to make. Several studies [177,178] reported the interactions of proteins with immobilized metal ions and compared various isotherm models such as the Langmuir model, the Freundlich model, the Tempkin model and the Langmuir-Freundlich model. Although the first three models were applicable for some systems, the authors concluded that the Langmuir-Freundlich model was the most efficient to explain the interactions of proteins with IMAC-M(II) gels. Indeed, this latter model considers the binding sites heterogeneity and the fact that adsorption energy of sites is different [179].

On the contrary, the Langmuir model—used to fit protein binding adsorption and determine the thermodynamic properties such as adsorption equilibrium constant and adsorption free energy—may induce error according to Latour [180]. Even if the shapes look similar [181,182], the protein binding isotherm may not fit all the required conditions to be a Langmuir model. Indeed, for using a Langmuir model, all binding sites must be identical, equivalent and independent, and have the same adsorption energy. More, Langmuir model needs a monolayer surface coverage and finally, no modifications and no interactions between already adsorbed species [183]. In addition, other parameters such as the ionic strength can affect the equilibrium characteristics of protein adsorption. Thus, Lan and co-workers [181] proposed a modified Langmuir model to take this ionic strength into account. Despite this, the Langmuir model is still widely used to fit adsorption data due to its simplicity and ease of use [178,182,184].

Furthermore, Vunnum et al. [185] proposed an approach to model non-linear multi-component equilibrium for preparative IMAC chromatography applied to proteins, considering the "multi-pointed" nature of adsorption upon binding of macromolecules, the possibility of steric hindrance, and the role of the mobile phase modifier.

A crucial point concerns the methodology for determining the model parameters, which vary according to the model chosen (for example q_{max} and K_A for a Langmuir model described by Equation (4)), and notably those involved in the adsorption isotherm as reviewed elsewhere [8]. Schmidt-Traub [163] defined three categories of methods: static methods (e.g., batch), dynamic methods (e.g., frontal analysis) or the determination of component interactions from single-component isotherms.

Concerning peptides, the experimental determination of the adsorption isotherm parameters may be difficult due to their high cost. Hence, the quantity of peptide needed

constitutes a criterion for the choice of the method to use, which explains the promising use of SPR biosensor. Several studies illustrate the complementarity and analogies of the information obtained by chromatography and biosensors. Arnell and co-workers [186] performed an analytical characterization of chiral drug-protein interactions by comparing SPR and the HPLC perturbation method. Agmo Hernández and colleagues [11] showed that numerical processing of liquid chromatography and biosensor data provided a better understanding of interactions with the adsorption medium.

Recently, our team [160] proposed an approach to determine the parameters of the mono- or multi-component Langmuir isotherm in IMAC chromatography from parameters measured in SPR. The mono component Langmuir equation is expressed by Equation (4) [187,188]:

$$q = \frac{q_{max} K_A C}{1 + K_A C} \quad (4)$$

where q_{max} is the maximal capacity (g/L stationary phase), K_A is the affinity constant (L/g) and C the concentration of solute in the mobile phase (g/L mobile phase).

For low peptide concentrations in the mobile phase, the slope of this isotherm corresponds to the product $q_{max} K_A$. It expresses the affinity of peptides on the metal ion sites and is assumed to be independent of the geometry of the surface on which the peptides are adsorbed (SPR planar chip vs. IMAC spherical particle) [160].

However, for better simulation, the competition between components in adsorption must be especially considered when imidazole is used for peptide elution; in this case, the multi-component Langmuir isotherm is expressed by Equation (5) [8]:

$$q_i = \frac{q_{max,i} K_{A,i} C_i}{1 + \sum_{i=1,n} K_{A,j} C_j} \quad (5)$$

$q_{max,i}$ and $K_{A,i}$ are determined in mono-constituent conditions.

In order to study the proof of concept of the SPR-IMAC analogy, our team [160] first performed simulations considering:

$$q_{max,IMAC} = q_{max,SPR} = q_{max} \quad (6)$$

$$K_{A,IMAC} = \frac{K_{A,SPR}}{MW} \quad (7)$$

where $K_{A,IMAC}$ expressed in L/g is estimated from a simple conversion of $K_{A,SPR}$ expressed in M^{-1} using the molecular weight (MW, g/mole) of the investigated peptide.

Simulations led to close simulated and experimental retention time (t_R). As far as low concentration injections are concerned (linear part of the sorption isotherm), these results allowed to validate the slope at the origin of the isotherm, corresponding to the product $K_{A,IMAC} * q_{max,IMAC}$. However, further work is needed to study $K_{A,IMAC}$ and $q_{max,IMAC}$ values independently. One approach could be to consider that the ratio $q_{max,IMAC}/q_{max,SPR}$ should not change significantly for a molecule investigated [160].

4.3.3. Axially Dispersed Plug Flow Model or Transport-Dispersive Model

The transport-dispersive model describes the mass transfer inside the column, assuming isothermal adsorption, radial homogeneity and lumped coefficients for axial dispersion and mass transfer resistances [13,164,189–194].

The mass balance for the mobile phase leads to the following continuity Equation (8):

$$\frac{\partial C_i}{\partial t} + \frac{1 - \varepsilon_T}{\varepsilon_T} \frac{\partial q_i}{\partial t} + \frac{u}{\varepsilon_T} \frac{\partial C_i}{\partial z} = D_L \frac{\partial^2 C_i}{\partial z^2} \forall i 1, 2, \ldots, N_c \text{ and } z \in (0, L) \quad (8)$$

where t is the time coordinate (s), z the axial coordinate (m), ε_T the total porosity, u the superficial velocity (m/s), D_L the apparent axial dispersion coefficient (m^2/s), N_c the

number of components in the system and L is the column length (m). In this former Equation (8):

$\frac{1-\varepsilon_T}{\varepsilon_T}$ represents Vs/Vm, which is the phase ratio, where Vs and Vm are the volumes of stationary phase and mobile phase, respectively,

$\frac{\partial C_i}{\partial t}$ describes the accumulation in the mobile phase,

$\frac{1-\varepsilon_T}{\varepsilon_T}\frac{\partial q_i}{\partial t}$ describes the accumulation in the stationary phase,

$\frac{u}{\varepsilon_T}\frac{\partial C_i}{\partial z}$ describes the convective transport in the mobile phase,

and $D_L\frac{\partial^2 C_i}{\partial z^2}$ describes the transport by axial dispersion in the mobile phase.

A way to solve Equation (8) relies on the ideal chromatography concepts. These ones rely on following assumptions: (i) the axial dispersion is neglected, (ii) all kinetic factors (i.e., mass transfer and kinetic resistance to binding) are considered fast enough to enable the mobile and stationary phases to be in equilibrium, (iii) the system is isothermal and isochore, (iv) the flow is one directional and constant volumetric, (v) porosity is constant and (vi) there is no channeling. Initially introduced by Glueckauf [195], this theory was then developed by several studies [196,197].

In a mono-constituent system or in the case of a system composed by many constituents that adsorb independently, the equilibrium theory and Equation (8) enable to express the migration velocity of the concentration of the constituent i (Ci) by Equation (9):

$$u_{C_i} = \left(\frac{\partial z}{\partial t}\right)_{C_i} = \frac{u}{1 + \frac{1-\varepsilon}{\varepsilon}\frac{dq_i}{dC_i}} \quad (9)$$

In the particular case of a linear isotherm where

$$q_i = K_i C_i \quad (10)$$

K_i being the slope of the isotherm, upon an injection, the retention time can thus be expressed by Equation (11):

$$t_R = \frac{L}{u_{C_i}} = \frac{L}{u}\left(1 + \frac{1-\varepsilon}{\varepsilon}K_i\right) \quad (11)$$

with u_{Ci} concentration velocity (ms^{-1}), u velocity of the mobile phase (ms^{-1}), ε the porosity (without unit), t_R retention time (s^{-1}) and L column length (m).

In the case of peptides, at low concentration, dq_i/dC_i tends towards the slope of the sorption isotherm plotted at the origin, which is equal to the product $K_{A,IMAC}$*$q_{max,IMAC}$. The higher this latter slope, the smaller the concentration velocity, and thus, t_R increases.

Note that the ideal chromatography concepts lead to the best potential separation. However, for columns design, it is necessary to consider the real performances, especially for biomolecules. Apart from few exceptions, kinetic resistance is rarely the rate-limiting step [198]. In proteins adsorption, the mass transfer is rather the limiting step due to their high molecular weight and their slow diffusion in solutions, despite their high affinity to most of the adsorption surfaces [180]. The mass transfer resistance can be either external, in the film surrounding the stationary phase, or internal, within the stationary phase. In the case of protein chromatography, the external transport is rarely the controlling and limiting mechanism [198]. In comparison to proteins, this mass transfer limitation should be less marked when studying peptides, in particular for bioactive peptides, which are small-in size.

When the rate-limiting step is the internal mass transfer, the accumulation term in the solid phase can be expressed using a simplified Linear Driving Force (LDF) type relationship, given by Equation (12).

$$\frac{\partial q_i}{\partial t} = k_m(q_i^* - q_i) \quad (12)$$

where k_m is the lumped mass transfer coefficient (s^{-1}), and q_i^*(g/L) is the solute concentration in the stationary phase at equilibrium as defined by the adsorption equilibrium isotherm.

k_m could be calculated using an empirical correlation described in Equation (13):

$$k_m = k_{max}\left[S_1 + (1 - S_1)\left(1 - \frac{q_R}{q_{max,R}}\right)^{S_2}\right] \text{ where } 0 \leq S1 \leq 1 \text{ and } S2 > 0 \quad (13)$$

where k_{max} (s^{-1}) is the maximum lumped mass transfer coefficient, q_R (g/L) is the sum of all the retained solute concentrations in the stationary phase, $q_{max,R}$ (g/L) is the maximum binding capacity of all the retained solutes from the adsorption equilibrium isotherm, S_1 and S_2 (no unit) are the saturation dependent kinetic constant and order, respectively. However, k_m is taken as a constant when breakthrough curves are symmetric [199].

The apparent axial dispersion coefficient, D_L (m^2/s) is defined by an empirical correlation (Equation (14) [13,190].

$$D_L = \frac{uL}{2N_p} \quad (14)$$

where u is the velocity (ms^{-1}), and L, the column length (m) and N_p (no unit), the theoretical plate number.

The theoretical plate number (N_p) is experimentally estimated by measuring the peak width at half height from the chromatogram of an unretained small molecule.

For a given column length (L, in m), Np can also be evaluated by considering the Height Equivalent to a Theoretical Plate (HETP) defined as H (Equation (15)).

$$N_P = \frac{L}{H} \quad (15)$$

This H(m) parameter can be evaluated using generalized Van Deemter curves [198].

In order to solve the dispersive model equation (Equation (8)), various conditions at the boundaries and initial conditions are proposed. Generally, the column is initially equilibrated by loading buffer either pure or non-pure [164]; thus, the initial biomolecule concentration at a given point z in the mobile and stationary phases is equal to zero, regardless the chromatographic mode: C (t = 0, z) = 0; q (t = 0, z) = 0. However, the boundary conditions vary according to the chromatographic mode, which can be frontal, by displacement or elution [164]. For the elution mode at the inlet of the column (z = 0), convection and dispersion are considered [164,192,193,199], leading thus to the following Equation (16) (Danckwert boundaries condition):

$$\left.\frac{\partial C}{\partial z}\right|_{z=0} = \frac{u}{\varepsilon_T D_L}(C(t, z = 0) - C_f) \quad (16)$$

where $C_f \neq 0$ for $0 < t < tL$ and corresponds to the concentration of biomolecule in a mobile phase inside the column while C (t, z = 0) stands for the inlet concentration.

The space boundary condition for a closed system at the outlet of the column z = L and $t \geq 0$ is described by the Equation (17), where only the convective transport is considered.

$$\left.\frac{\partial C}{\partial z}\right|_{z=L} = 0 \quad (17)$$

The continuity equation (see Equation (8)) is solved numerically using various methods such as the finite difference based on Rouchon algorithms (backward-backward scheme) [135,200], the fast Fourier transform technique [164], the Newton's method or Picard iteration [189]. The Figure 5 summarizes the steps and parameters taken into consideration to simulate peptides concentration profiles at the column outlet vs. time, thus the simulation enables to study the conditions necessary for performing separation.

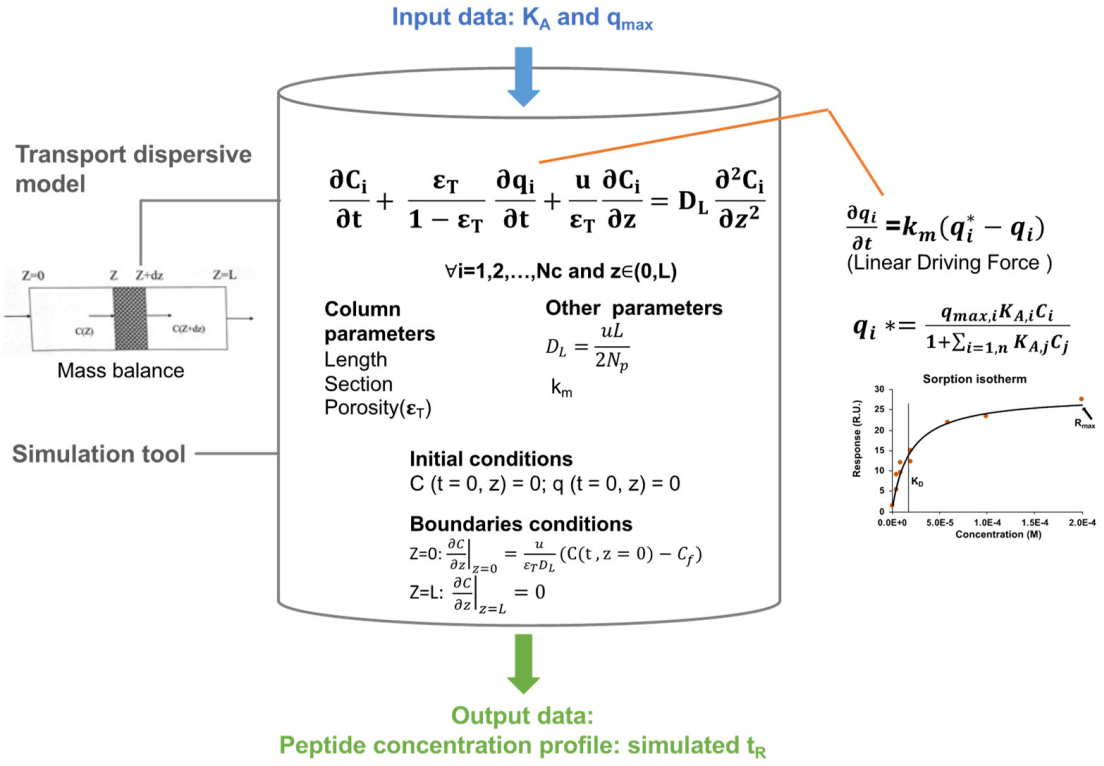

Figure 5. Chromatographic column modelling using transport dispersive model.

Furthermore, a chromatographic column can be also considered as a cascade of continuous stirred-tank reactors as well. This theory played an important role in chromatography development but were neither able to describe the peaks spreading phenomenon [164] nor to predict adsorption rate limitations [198], thus it will not be discussed in this work.

5. Conclusions

The separation of MCPs using IMAC is challenging due to the complexity of peptides mixtures of hydrolysates. Therefore, all the parameters affecting separation in IMAC need to be studied carefully in order to decide which metal, which complexing agent, which column and which buffers to use. The concomitant analyses by SPR and transport dispersive model to simulate MCPs separation will enable researchers and industries to do a preliminary study before launching experimental studies or process, thus reducing time and costs, number of experiments to perform and quantity of chemicals as well. Finally, as perspective, molecular dynamic simulation could be an interesting option to deepen the molecular insight into Immobilized Metal ion Affinity Chromatography.

Author Contributions: Writing original draft preparation: R.I. and J.A.C.E.; review and editing: C.P. and L.S.; writing, review and editing: K.S., L.M. and L.C.-R.; conceptualization, supervision, project administration: L.C.-R.; funding acquisition: S.D. and L.C.-R. All authors have read and agreed to the published version of the manuscript.

Funding: This research was funded by the French ministry government via the MESR PhD grant; the ANR JCJC MELISSA (2020–2024), the "Impact Biomolecules" project of the "Lorraine Université d'Excellence "(Investissements d'avenir–ANR project number 15–004) and the project ICEEL INTRA MELISSA 2019.

Data Availability Statement: Not applicable.

Conflicts of Interest: The authors declare no conflict of interest.

Abbreviations

AA: Amino Acid; C: Concentration of the solute in the mobile phase (M or g/L); CM-Asp: CarboxyMethylated aspartic acid; DH: Degree of Hydrolysis; D_L: apparent axial dispersion coefficient (m^2/s); HSAB: Hard and Soft Acids and Bases; IDA: IminoDiacetic Acid; IMAC: Immobilized Metal-ion Affinity Chromatography; K_A: Affinity constant (M-1 ou L/g); K_D: Constant of dissociation (M); L: column length(m); LHRH: Leuteinizing Hormone-Releasing Hormone; MCPs: Metal-Chelating Peptides; MW: molecular weight (g/mol); N_c: number of components in the system (without unit); NTA: NitriloTriacetic Acid; q: concentration of the solute in the stationary phase (g/L); q_{max}: maximum capacity (g/L); R: Response (RU); R_{max}: Maximum response; RU: Resonance Units; SPR: Surface Plasmon Resonance; t: time coordinate (s); TED: N,N,N′-tris(carboxymethyl) ethylene diamine; u: superficial velocity (m/s); UF: UltraFiltration; z: axial coordinate (m); ε_T: total porosity (without unit).

References

1. Guo, L.; Harnedy, P.A.; Li, B.; Hou, H.; Zhang, Z.; Zhao, X.; FitzGerald, R.J. Food protein-derived chelating peptides: Biofunctional ingredients for dietary mineral bioavailability enhancement. *Trends Food Sci. Technol.* **2014**, *37*, 92–105. [CrossRef]
2. Tu, M.; Cheng, S.; Lu, W.; Du, M. Advancement and prospects of bioinformatics analysis for studying bioactive peptides from food-derived protein: Sequence, structure, and functions. *Trac Trends Anal. Chem.* **2018**, *105*, 7–17. [CrossRef]
3. Chalamaiah, M.; Ulug, S.K.; Hong, H.; Wu, J. Regulatory requirements of bioactive peptides (protein hydrolysates) from food proteins. *J. Funct. Foods* **2019**, *58*, 123–129. [CrossRef]
4. Liu, L.; Li, S.; Zheng, J.; Bu, T.; He, G.; Wu, J. Safety considerations on food protein-derived bioactive peptides. *Trends Food Sci. Technol.* **2019**, *96*, 199–207. [CrossRef]
5. Wong, J.W.; Albright, R.L.; Wang, N.-H.L. Immobilized Metal Ion Affinity Chromatography (IMAC) Chemistry and Bioseparation Applications. *Sep. Purif. Methods* **1991**, *20*, 49–106. [CrossRef]
6. Cheung, R.C.F.; Wong, J.H.; Ng, T.B. Immobilized metal ion affinity chromatography: A review on its applications. *Appl. Microbiol. Biotechnol.* **2012**, *96*, 1411–1420. [CrossRef]
7. Lenz, K.; Beste, Y.A.; Arlt, W. Comparison of static and dynamic measurements of adsorption isotherms. *Sep. Sci. Technol.* **2002**, *37*, 1611–1629. [CrossRef]
8. Seidel-Morgenstern, A. Experimental determination of single solute and competitive adsorption isotherms. *J. Chromatogr. A* **2004**, *1037*, 255–272. [CrossRef]
9. Cornel, J.; Tarafder, A.; Katsuo, S.; Mazzotti, M. The direct inverse method: A novel approach to estimate adsorption isotherm parameters. *J. Chromatogr. A* **2010**, *1217*, 1934–1941. [CrossRef]
10. Silva, T.C.; Eppink, M.; Ottens, M. Small, smaller, smallest: Miniaturization of chromatographic process development. *J. Chromatogr. A* **2022**, *1681*, 463451. [CrossRef] [PubMed]
11. Hernández, V.A.; Samuelsson, J.; Forssén, P.; Fornstedt, T. Enhanced interpretation of adsorption data generated by liquid chromatography and by modern biosensors. *J. Chromatogr. A* **2013**, *1317*, 22–31. [CrossRef] [PubMed]
12. Canabady-Rochelle, L.L.; Selmeczi, K.; Collin, S.; Pasc, A.; Muhr, L.; Boschi-Muller, S. SPR screening of metal chelating peptides in a hydrolysate for their antioxidant properties. *Food Chem.* **2018**, *239*, 478–485. [CrossRef] [PubMed]
13. Guiochon, G.; Shirazi, D.G.; Felinger, A.; Katti, A.M. *Fundamentals of Preparative and Nonlinear Chromatography*; Academic Press: Boston, MA, USA, 2006.
14. Remelli, M.; Nurchi, V.M.; Lachowicz, J.I.; Medici, S.; Zoroddu, M.A.; Peana, M. Competition between Cd(II) and other divalent transition metal ions during complex formation with amino acids, peptides, and chelating agents. *Coord. Chem. Rev.* **2016**, *327–328*, 55–69. [CrossRef]
15. Wang, C.; Li, B.; Ao, J. Separation and identification of zinc-chelating peptides from sesame protein hydrolysate using IMAC-Zn2+ and LC–MS/MS. *Food Chem.* **2012**, *134*, 1231–1238. [CrossRef]
16. Guo, L.; Harnedy, P.A.; O'Keeffe, M.B.; Zhang, L.; Li, B.; Hou, H.; FitzGerald, R.J. Fractionation and identification of Alaska pollock skin collagen-derived mineral chelating peptides. *Food Chem.* **2015**, *173*, 536–542. [CrossRef] [PubMed]
17. Udechukwu, M.C.; Collins, S.A.; Udenigwe, C.C. Prospects of enhancing dietary zinc bioavailability with food-derived zinc-chelating peptides. *Food Funct.* **2016**, *7*, 4137–4144. [CrossRef] [PubMed]
18. Wu, W.; Yang, Y.; Sun, N.; Bao, Z.; Lin, S. Food protein-derived iron-chelating peptides: The binding mode and promotive effects of iron bioavailability. *Food Res. Int.* **2020**, *131*, 108976. [CrossRef]
19. Wen, C.; Zhang, J.; Zhang, H.; Duan, Y.; Ma, H. Plant protein-derived antioxidant peptides: Isolation, identification, mechanism of action and application in food systems: A review. *Trends Food Sci. Technol.* **2020**, *105*, 308–322. [CrossRef]
20. Gaetke, L. Copper toxicity, oxidative stress, and antioxidant nutrients. *Toxicology* **2003**, *189*, 147–163. [CrossRef]
21. Chalamaiah, M.; Yu, W.; Wu, J. Immunomodulatory and anticancer protein hydrolysates (peptides) from food proteins: A review. *Food Chem.* **2017**, *245*, 205–222. [CrossRef]
22. Di Natale, C.; De Benedictis, I.; De Benedictis, A.; Marasco, D. Metal–Peptide Complexes as Promising Antibiotics to Fight Emerging Drug Resistance: New Perspectives in Tuberculosis. *Antibiotics* **2020**, *9*, 337. [CrossRef] [PubMed]

23. Csire, G.; Canabady-Rochelle, L.; Averlant-Petit, M.-C.; Selmeczi, K.; Stefan, L. Both metal-chelating and free radical-scavenging synthetic pentapeptides as efficient inhibitors of reactive oxygen species generation. *Metallomics* **2020**, *12*, 1220–1229. [CrossRef] [PubMed]
24. Csire, G.; Dupire, F.; Canabady-Rochelle, L.; Selmeczi, K.; Stefan, L. Bio-Inspired Casein-Derived Antioxidant Peptides Exhibiting a Dual Direct/Indirect Mode of Action. *Inorg. Chem.* **2022**, *61*, 1941–1948. [CrossRef] [PubMed]
25. Nwachukwu, I.D.; Aluko, R.E. Structural and functional properties of food protein-derived antioxidant peptides. *J. Food Biochem.* **2019**, *43*, e12761. [CrossRef]
26. Sarbon, N.M.; Badii, F.; Howell, N.K. Purification and characterization of antioxidative peptides derived from chicken skin gelatin hydrolysate. *Food Hydrocoll.* **2018**, *85*, 311–320. [CrossRef]
27. Sun, N.; Wu, H.; Du, M.; Tang, Y.; Liu, H.; Fu, Y.; Zhu, B. Food protein-derived calcium chelating peptides: A review. *Trends Food Sci. Technol.* **2016**, *58*, 140–148. [CrossRef]
28. Harnedy, P.A.; FitzGerald, R.J. Bioactive peptides from marine processing waste and shellfish: A review. *J. Funct. Foods* **2012**, *4*, 6–24. [CrossRef]
29. Rahman, M.; Khalid, H.S.; Akhtar, M.F.; Ijaz, M.; Iqbal, M.; Bukhari, S.A.; Mustafa, G.; Shaukat, K. *Handbook of Bioremediation*; Elsevier: Amsterdam, The Netherlands, 2021; pp. 437–444.
30. Carlton, D.D., Jr.; Schug, K.A. A review on the interrogation of peptide–metal interactions using electrospray ionization-mass spectrometry. *Analytica Chimica Acta* **2011**, *68*, 19–39. [CrossRef]
31. Jung, W.-K.; Karawita, R.; Heo, S.-J.; Lee, B.-J.; Kim, S.-K.; Jeon, Y.-J. Recovery of a novel Ca-binding peptide from Alaska Pollack (*Theragra chalcogramma*) backbone by pepsinolytic hydrolysis. *Process Biochem.* **2006**, *41*, 2097–2100. [CrossRef]
32. Storcksdieck, S.; Bonsmann, S.S.G.; Hurrell, R.F. Iron-Binding Properties, Amino Acid Composition, and Structure of Muscle Tissue Peptides from in vitro Digestion of Different Meat Sources. *J. Food Sci.* **2007**, *72*, S019–S029. [CrossRef]
33. Lee, S.H. Isolation of a Calcium-binding Peptide from Enzymatic Hydrolysates of Porcine Blood Plasma Protein. *J. Korean Soc. Appl. Biol. Chem.* **2009**, *52*, 290–294. [CrossRef]
34. Huang, S.-L.; Zhao, L.-N.; Cai, X.; Wang, S.-Y.; Huang, Y.-F.; Hong, J.; Rao, P.-F. Purification and characterisation of a glutamic acid-containing peptide with calcium-binding capacity from whey protein hydrolysate. *J. Dairy Res.* **2015**, *82*, 29–35. [CrossRef] [PubMed]
35. Hou, Y.; Wu, Z.; Dai, Z.; Wang, G.; Wu, G. Protein hydrolysates in animal nutrition: Industrial production, bioactive peptides, and functional significance. *J. Anim. Sci. Biotechnol.* **2017**, *8*, 1–13. [CrossRef] [PubMed]
36. Chen, D.; Liu, Z.; Huang, W.; Zhao, Y.; Dong, S.; Zeng, M. Purification and characterisation of a zinc-binding peptide from oyster protein hydrolysate. *J. Funct. Foods* **2013**, *5*, 689–697. [CrossRef]
37. Wu, H.; Liu, Z.; Zhao, Y.; Zeng, M. Enzymatic preparation and characterization of iron-chelating peptides from anchovy (*Engraulis japonicus*) muscle protein. *Food Res. Int.* **2012**, *48*, 435–441. [CrossRef]
38. Charoenphun, N.; Cheirsilp, B.; Sirinupong, N.; Youravong, W. Calcium-binding peptides derived from tilapia (*Oreochromis niloticus*) protein hydrolysate and its calcium bioavailability in rats. *J. Funct. Foods* **2012**, *236*, 57–63. [CrossRef]
39. Miao, J.; Liao, W.; Pan, Z.; Wang, Q.; Duan, S.; Xiao, S.; Yang, Z.; Cao, Y. Isolation and identification of iron-chelating peptides from casein hydrolysates. *Food Funct.* **2019**, *10*, 2372–2381. [CrossRef]
40. Timón, M.L.; Andrés, A.I.; Otte, J.; Petrón, M.J. Antioxidant peptides (<3 kDa) identified on hard cow milk cheese with rennet from different origin. *Food Res. Int.* **2019**, *120*, 643–649. [CrossRef]
41. Nielsen, S.D.; Beverly, R.L.; Qu, Y.; Dallas, D.C. Milk bioactive peptide database: A comprehensive database of milk protein-derived bioactive peptides and novel visualization. *Food Chem.* **2017**, *232*, 673–682. [CrossRef]
42. Choi, D.-W.; Lee, J.-H.; Chun, H.-H.; Bin Song, K. Isolation of a calcium-binding peptide from bovine serum protein hydrolysates. *Food Sci. Biotechnol.* **2012**, *21*, 1663–1667. [CrossRef]
43. Zhao, L.; Huang, S.; Cai, X.; Hong, J.; Wang, S. A specific peptide with calcium chelating capacity isolated from whey protein hydrolysate. *J. Funct. Foods* **2014**, *10*, 46–53. [CrossRef]
44. Megías, C.; Pedroche, J.; Yust, M.M.; Girón-Calle, J.; Alaiz, M.; Millán, F.; Vioque, J. Production of copper-chelating peptides after hydrolysis of sunflower proteins with pepsin and pancreatin. *LWT* **2008**, *41*, 1973–1977. [CrossRef]
45. Lv, Y.; Bao, X.; Liu, H.; Ren, J.; Guo, S. Purification and characterization of caclium-binding soybean protein hydrolysates by Ca2+/Fe3+ immobilized metal affinity chromatography (IMAC). *Food Chem.* **2013**, *141*, 1645–1650. [CrossRef]
46. Liu, F.-R.; Wang, L.; Wang, R.; Chen, Z.-X. Calcium-Binding Capacity of Wheat Germ Protein Hydrolysate and Characterization of Peptide–Calcium Complex. *J. Agric. Food Chem.* **2013**, *61*, 7537–7544. [CrossRef]
47. Eckert, E.; Lu, L.; Unsworth, L.D.; Chen, L.; Xie, J.; Xu, R. Biophysical and in vitro absorption studies of iron chelating peptide from barley proteins. *J. Funct. Foods* **2016**, *25*, 291–301. [CrossRef]
48. Budseekoad, S.; Yupanqui, C.T.; Sirinupong, N.; Alashi, A.M.; Aluko, R.E.; Youravong, W. Structural and functional characterization of calcium and iron-binding peptides from mung bean protein hydrolysate. *J. Funct. Foods* **2018**, *49*, 333–341. [CrossRef]
49. Aryee, A.N.A.; Boye, J.I. Improving the Digestibility of Lentil Flours and Protein Isolate and Characterization of Their Enzymatically Prepared Hydrolysates. *Int. J. Food Prop.* **2016**, *19*, 2649–2665. [CrossRef]
50. Hadnadjev, M.; Dapcevic-Hadnadjev, T.; Pojic, M.; Saric, B.; Misan, A.; Jovanov, P.; Sakac, M. Progress in vegetable proteins isolation techniques: A review. *Food Feed Res.* **2017**, *44*, 11–21. [CrossRef]

51. Udenigwe, C.; Aluko, R.E. Food Protein-Derived Bioactive Peptides: Production, Processing, and Potential Health Benefits. *J. Food Sci.* **2011**, *77*, R11–R24. [CrossRef]
52. Chen, D.; Mu, X.; Huang, H.; Nie, R.; Liu, Z.; Zeng, M. Isolation of a calcium-binding peptide from tilapia scale protein hydrolysate and its calcium bioavailability in rats. *J. Funct. Foods* **2014**, *6*, 575–584. [CrossRef]
53. Wu, W.; Li, B.; Hou, H.; Zhang, H.; Zhao, X. Identification of iron-chelating peptides from Pacific cod skin gelatin and the possible binding mode. *J. Funct. Foods* **2017**, *35*, 418–427. [CrossRef]
54. Jiang, H.; Zhang, W.; Chen, F.; Zou, J.; Chen, W.; Huang, G. Purification of an iron-binding peptide from scad (*Decapterus maruadsi*) processing by-products and its effects on iron absorption by Caco-2 cells. *J. Food Biochem.* **2019**, *43*, e12876. [CrossRef] [PubMed]
55. Malison, A.; Arpanutud, P.; Keeratipibul, S. Chicken foot broth byproduct: A new source for highly effective peptide-calcium chelate. *Food Chem.* **2020**, *345*, 128713. [CrossRef] [PubMed]
56. Xie, N.; Huang, J.; Li, B.; Cheng, J.; Wang, Z.; Yin, J.; Yan, X. Affinity purification and characterisation of zinc chelating peptides from rapeseed protein hydrolysates: Possible contribution of characteristic amino acid residues. *Food Chem.* **2015**, *173*, 210–217. [CrossRef] [PubMed]
57. Guo, L.; Hou, H.; Li, B.; Zhang, Z.; Wang, S.; Zhao, X. Preparation, isolation and identification of iron-chelating peptides derived from Alaska pollock skin. *Process Biochem.* **2013**, *48*, 988–993. [CrossRef]
58. Hou, H.; Wang, S.; Zhu, X.; Li, Q.; Fan, Y.; Cheng, D.; Li, B. A novel calcium-binding peptide from Antarctic krill protein hydrolysates and identification of binding sites of calcium-peptide complex. *Food Chem.* **2018**, *243*, 389–395. [CrossRef]
59. Lv, Y.; Wei, K.; Meng, X.; Huang, Y.; Zhang, T.; Li, Z. Separation and identification of iron-chelating peptides from defatted walnut flake by nanoLC-ESI–MS/MS and de novo sequencing. *Process Biochem.* **2017**, *59*, 223–228. [CrossRef]
60. Zhang, F.; Qu, J.; Thakur, K.; Zhang, J.-G.; Mocan, A.; Wei, Z.-J. Purification and identification of an antioxidative peptide from peony (*Paeonia suffruticosa* Andr.) seed dreg. *Food Chem.* **2019**, *285*, 266–274. [CrossRef]
61. Daroit, D.J.; Brandelli, A. In vivo bioactivities of food protein-derived peptides–a current review. *Curr. Opin. Food Sci.* **2021**, *39*, 120–129. [CrossRef]
62. Daliri, E.; Oh, D.; Lee, B. Bioactive Peptides. *Foods* **2017**, *6*, 32. [CrossRef]
63. Korhonen, H.; Pihlanto, A. Food-derived Bioactive Peptides-Opportunities for Designing Future Foods. *Curr. Pharm. Des.* **2003**, *9*, 1297–1308. [CrossRef] [PubMed]
64. Conti, J.P.; Vinderola, G.; Esteban, E.N. Characterization of a soy protein hydrolyzate for the development of a functional ingredient. *J. Food Sci. Technol.* **2019**, *56*, 896–904. [CrossRef] [PubMed]
65. Lorenzo, J.M.; Munekata, P.E.; Gómez, B.; Barba, F.J.; Mora, L.; Pérez-Santaescolástica, C.; Toldrá, F. Bioactive peptides as natural antioxidants in food products–A review. *Trends Food Sci. Technol.* **2018**, *79*, 136–147. [CrossRef]
66. Beaubier, S.; Framboisier, X.; Fournier, F.; Galet, O.; Kapel, R. A new approach for modelling and optimizing batch enzymatic proteolysis. *Chem. Eng. J.* **2020**, *405*, 126871. [CrossRef]
67. Dash, P.; Ghosh, G. Amino acid composition, antioxidant and functional properties of protein hydrolysates from Cucurbitaceae seeds. *J. Food Sci. Technol.* **2017**, *54*, 4162–4172. [CrossRef] [PubMed]
68. Adler-Nissen, J. *Enzymic Hydrolysis of Food Proteins*; Elsevier: Amsterdam, The Netherlands, 1986.
69. Gutiérrez, R.; Del Valle, E.M.M.; Galán, M.A. Immobilized Metal-Ion Affinity Chromatography: Status and Trends. *Sep. Purif. Rev.* **2007**, *36*, 71–111. [CrossRef]
70. Pearson, R.G. Hard and Soft Acids and Bases. *J. Am. Chem. Soc.* **1963**, *85*, 3533–3539. [CrossRef]
71. Melnikov, F.; Geohagen, B.C.; Gavin, T.; LoPachin, R.M.; Anastas, P.T.; Coish, P.; Herr, D.W. Application of the hard and soft, acids and bases (HSAB) theory as a method to predict cumulative neurotoxicity. *Neuro Toxicol.* **2020**, *79*, 95–103. [CrossRef]
72. Kozłowski, H.; Bal, W.; Dyba, M.; Kowalik-Jankowska, T. Specific structure–stability relations in metallopeptides. *Coord. Chem. Rev.* **1999**, *184*, 319–346. [CrossRef]
73. Sóvágó, I.; Várnagy, K.; Lihi, N.; Grenács. Coordinating properties of peptides containing histidyl residues. *Coord. Chem. Rev.* **2016**, *327*, 43–54. [CrossRef]
74. Wątły, J.; Hecel, A.; Rowińska-Żyrek, M.; Kozłowski, H. Impact of histidine spacing on modified polyhistidine tag–Metal ion interactions. *Inorganica Chim. Acta* **2018**, *472*, 119–126. [CrossRef]
75. Watly, J.; Simonovsky, E.; Wieczorek, R.; Barbosa, N.; Miller, Y.; Kozlowski, H. Insight into the Coordination and the Binding Sites of Cu^{2+} by the Histidyl-6-Tag using Experimental and Computational Tools. *Inorg. Chem.* **2014**, *53*, 6675–6683. [CrossRef] [PubMed]
76. Yamauchi, O.; Odani, A. Stability constants of metal complexes of amino acids with charged side chains-Part I: Positively charged side chains (Technical Report). *Pure Appl. Chem.* **1996**, *68*, 469–496. [CrossRef]
77. Everson, R.; Parker, H. Zinc binding and synthesis of eight-hydroxy-quinoline-agarose. *Bioinorg. Chem.* **1974**, *4*, 15–20. [CrossRef]
78. Porath, J.; Carlsson, J.; Olsson, I.; Belfrage, G. Metal chelate affinity chromatography, a new approach to protein fractionation. *Nature* **1975**, *258*, 598–599. [CrossRef]
79. Sun, X.; Chiu, J.-F.; He, Q.-Y. Application of immobilized metal affinity chromatography in proteomics. *Expert Rev. Proteom.* **2005**, *2*, 649–657. [CrossRef]
80. Tsai, S.-Y.; Lin, S.-C.; Suen, S.-Y.; Hsu, W.-H. Effect of number of poly(His) tags on the adsorption of engineered proteins on immobilized metal affinity chromatography adsorbents. *Process Biochem.* **2006**, *41*, 2058–2067. [CrossRef]

81. Chaga, G.S. Twenty-five years of immobilized metal ion affinity chromatography: Past, present and future. *J. Biochem. Biophys. Methods* **2001**, *49*, 313–334. [CrossRef]
82. Ueda, E.; Gout, P.; Morganti, L. Current and prospective applications of metal ion–protein binding. *J. Chromatogr. A* **2003**, *988*, 1–23. [CrossRef]
83. Michalski, W.P. Resolution of three forms of superoxide dismutase by immobilised metal affinity chromatography. *J. Chromatogr. B Biomed. Sci. Appl.* **1992**, *576*, 340–345. [CrossRef]
84. Biswas, S.; Sarkar, A.; Misra, R. Iron affinity gel and gallium immobilized metal affinity chromatographic technique for phosphopeptide enrichment: A comparative study. *Biotechnol. Biotechnol. Equip.* **2017**, *31*, 639–646. [CrossRef]
85. Abelin, J.G.; Trantham, P.D.; Penny, S.A.; Patterson, A.; Ward, S.; Hildebrand, W.H.; Cobbold, M.; Bai, D.L.; Shabanowitz, J.; Hunt, D.F. Complementary IMAC enrichment methods for HLA-associated phosphopeptide identification by mass spectrometry. *Nat. Protoc.* **2015**, *10*, 1308–1318. [CrossRef]
86. Ruprecht, B.; Koch, H.; Medard, G.; Mundt, M.; Kuster, B.; Lemeer, S. Comprehensive and Reproducible Phosphopeptide Enrichment Using Iron Immobilized Metal Ion Affinity Chromatography (Fe-IMAC) Columns. *Mol. Cell. Proteom.* **2015**, *14*, 205–215. [CrossRef] [PubMed]
87. Barron, L.; O'Toole, M.; Diamond, D.; Nesterenko, P.N.; Paull, B. Separation of transition metals on a poly-iminodiacetic acid grafted polymeric resin column with post-column reaction detection utilising a paired emitter–detector diode system. *J. Chromatogr. A* **2008**, *1213*, 31–36. [CrossRef] [PubMed]
88. Ross, A.R.; Ikonomou, M.G.; Orians, K.J. Characterization of copper-complexing ligands in seawater using immobilized copper(II)-ion affinity chromatography and electrospray ionization mass spectrometry. *Mar. Chem.* **2003**, *83*, 47–58. [CrossRef]
89. Gu, J.; Codd, R. The resolution of two clinical agents, bleomycin and desferrioxamine B, from a Streptomyces verticillus fermentation mixture using multi-dimensional immobilised metal ion affinity chromatography. *RSC Adv.* **2014**, *5*, 3443–3453. [CrossRef]
90. Simionato, A.V.C.; Silva-Stenico, M.E.; Tsai, S.M.; Carrilho, E. Evidences of siderophores synthesis by Grapevine Xylella fastidiosa, causal agent of pierce's disease, through instrumental approaches. *J. Braz. Chem. Soc.* **2010**, *21*, 635–641. [CrossRef]
91. Hu, Y.; Guo, S.; Li, X.; Ren, X. Comparative analysis of salt-responsive phosphoproteins in maize leaves using Ti 4+ -IMAC enrichment and ESI-Q-TOFMS: Proteomics and 2DE. *Electrophoresis* **2013**, *34*, 485–492. [CrossRef]
92. Rodrigues, C.A.; Reynaud, F.; Stadler, E.; Drago, V. Preparation, Characterization, and Chromatography Properties of Chitin Modified with $FeCl_3$. *J. Liq. Chromatogr. Relat. Technol.* **1999**, *22*, 761–769. [CrossRef]
93. Bonn, G.K.; Kalghatgi, K.; Horne, W.C.; Horváth, C. Rapid metal-interaction chromatography of proteins and peptides on micropellicular sorbents. *Chromatographia* **1990**, *30*, 484–488. [CrossRef]
94. Burba, P.; Jakubowski, B.; Kuckuk, R.; Küllmer, K.; Heumann, K.G. Characterization of aquatic humic substances and their metal complexes by immobilized metal-chelate affinity chromatography on iron(III)-loaded ion exchangers. *Anal. Bioanal. Chem.* **2000**, *368*, 689–696. [CrossRef] [PubMed]
95. de Aquino, L.C.L.; de Sousa, H.R.T.; Miranda, E.A.; Vilela, L.; Bueno, S.M.A. Evaluation of IDA-PEVA hollow fiber membrane metal ion affinity chromatography for purification of a histidine-tagged human proinsulin. *J. Chromatogr. B* **2006**, *834*, 68–76. [CrossRef] [PubMed]
96. Ortiz-Martin, L.; Benavente, F.; Medina-Casanellas, S.; Giménez, E.; Sanz-Nebot, V. Study of immobilized metal affinity chromatography sorbents for the analysis of peptides by on-line solid-phase extraction capillary electrophoresis-mass spectrometry: CE and CEC. *Electrophoresis* **2015**, *36*, 962–970. [CrossRef] [PubMed]
97. Sulkowski, E. Purification of proteins by IMAC. *Trends Biotechnol.* **1985**, *3*, 1–7. [CrossRef]
98. Del Contreras, M.M.; Lama-Muñoz, A.; Manuel Gutiérrez-Pérez, J.; Espínola, F.; Moya, M.; Castro, E. Protein extraction from agri-food residues for integration in biorefinery: Potential techniques and current status. *Bioresour. Technol.* **2019**, *280*, 459–477. [CrossRef]
99. Pavan, G.L.; Bresolin, I.; Borsoi-Ribeiro, M.; Vijayalakshmi, M.; Bueno, S.M.A. The effect of NaCl on the adsorption of human IgG onto CM-Asp–PEVA hollow fiber membrane-immobilized nickel and cobalt metal ions. *Adsorption* **2014**, *20*, 677–688. [CrossRef]
100. Gladilovich, V.; Greifenhagen, U.; Sukhodolov, N.; Selyutin, A.; Singer, D.; Thieme, D.; Majovsky, P.; Shirkin, A.; Hoehenwarter, W.; Bonitenko, E.; et al. Immobilized metal affinity chromatography on collapsed Langmuir-Blodgett iron(III) stearate films and iron(III) oxide nanoparticles for bottom-up phosphoproteomics. *J. Chromatogr. A* **2016**, *1443*, 181–190. [CrossRef]
101. De Góes, L.C.; Miranda, E.A.; Bueno, S.M.A. Interaction of histidine-tagged human proinsulin with immobilized nickel ion: Effect of chelating ligand and thermodynamics analysis. *Colloids Surf. A Physicochem. Eng. Asp.* **2010**, *369*, 176–185. [CrossRef]
102. Block, H.; Maertens, B.; Spriestersbach, A.; Brinker, N.; Kubicek, J.; Fabis, R.; Labahn, J.; Schäfer, F. *Methods in Enzymology*; Elsevier: Amsterdam, The Netherlands, 2009; pp. 439–473.
103. Hochuli, E. Genetically designed affinity chromatography using a novel metal chelate adsorben. *Biol. Active Mol.* **1989**, *411*, 217–239.
104. Smith, M.C.; Furman, T.C.; Ingolia, T.D.; Pidgeon, C. Chelating peptide-immobilized metal ion affinity chromatography. A new concept in affinity chromatography for recombinant proteins. *J. Biol. Chem.* **1988**, *263*, 7211–7215. [CrossRef]
105. Paris, C. *Developpement de Nouvelles Approches Analytiques Pour le Criblage de Peptides Chelateurs de fer*; Université de Lorraine: Lorraine, France, 2021.

106. Nuwaysir, L.M.; Stults, J.T. Electrospray ionization mass spectrometry of phosphopeptides isolated by on-line immobilized metal-ion affinity chromatography. *J. Am. Soc. Mass Spectrom.* **1993**, *4*, 662–669. [CrossRef]
107. Wang, J.; Zhang, Y.; Jiang, H.; Cai, Y.; Qian, X. Phosphopeptide detection using automated online IMAC-capillary LC-ESI-MS/MS. *Proteomics* **2006**, *6*, 404–411. [CrossRef] [PubMed]
108. Moser, K.; White, F. Phosphoproteomic Analysis of Rat Liver by High Capacity IMAC and LC−MS/MS. *J. Proteome Res.* **2005**, *5*, 98–104. [CrossRef] [PubMed]
109. Lv, Y.; Liu, Q.; Bao, X.; Tang, W.; Yang, B.; Guo, S. Identification and Characteristics of Iron-Chelating Peptides from Soybean Protein Hydrolysates Using IMAC-Fe^{3+}. *J. Agric. Food Chem.* **2009**, *57*, 4593–4597. [CrossRef]
110. Ejje, N.; Soe, C.Z.; Gu, J.; Codd, R. The variable hydroxamic acid siderophore metabolome of the marine actinomycete Salinispora tropica CNB-440. *Metallomics* **2013**, *5*, 1519–1528. [CrossRef]
111. Braich, N.; Codd, R. Immobilised metal affinity chromatography for the capture of hydroxamate-containing siderophores and other Fe(iii)-binding metabolites directly from bacterial culture supernatants. *Analyst* **2008**, *133*, 877–880. [CrossRef]
112. Bresolin, I.R.A.P.; Bresolin, I.T.L.; Pessoa, A. Purification of Anti-Interleukin-6 Monoclonal Antibody Using Precipitation and Immobilized Metal-Ion Affinity Chromatography. *Adsorpt. Sci. Technol.* **2015**, *33*, 191–202. [CrossRef]
113. Li, S.; Dass, C. Iron(III)-Immobilized Metal Ion Affinity Chromatography and Mass Spectrometry for the Purification and Characterization of Synthetic Phosphopeptides. *Anal. Biochem.* **1999**, *270*, 9–14. [CrossRef]
114. Lee, J.; Xu, Y.; Chen, Y.; Sprung, R.; Kim, S.C.; Xie, S.; Zhao, Y. Mitochondrial Phosphoproteome Revealed by an Improved IMAC Method and MS/MS/MS. *Mol. Cell. Proteom.* **2007**, *6*, 669–676. [CrossRef]
115. de la Hoz, L.; Ponezi, A.N.; Milani, R.F.; da Silva, V.S.N.; de Souza, A.S.; Bertoldo-Pacheco, M.T. Iron-binding properties of sugar cane yeast peptides. *Food Chem.* **2014**, *142*, 166–169. [CrossRef]
116. Duhita, N.; Hiwasa-Tanase, K.; Yoshida, S.; Ezura, H. Single-Step Purification of Native Miraculin Using Immobilized Metal-Affinity Chromatography. *J. Agric. Food Chem.* **2009**, *57*, 5148–5151. [CrossRef] [PubMed]
117. Gonzalez-Ortega, O.; Guzmán, R. Purification of Human Serum Immunoglobulins Using Immobilized Metal Affinity Chromatography with Ethylenediamine Triacetic Acid as Chelating Agent. *J. Liq. Chromatogr. Relat. Technol.* **2014**, *38*, 74–81. [CrossRef]
118. Hutchens, T.W.; Li, C.M. Estrogen receptor interaction with immobilized metals: Differential molecular recognition of Zn2+, Cu2+ and Ni2+ and separation of receptor isoforms. *J. Mol. Recognit.* **1988**, *1*, 80–92. [CrossRef] [PubMed]
119. Vançan, S.; Miranda, E.A.; Bueno, S.M.A. IMAC of human IgG: Studies with IDA-immobilized copper, nickel, zinc, and cobalt ions and different buffer systems. *Process Biochem.* **2002**, *37*, 573–579. [CrossRef]
120. Rowinska-Zyrek, M.; Witkowska, D.; Potocki, S.; Remelli, M.; Kozlowski, H. His-rich sequences–is plagiarism from nature a good idea? *N. J. Chem.* **2013**, *37*, 58–70. [CrossRef]
121. He, Z.; Tan, J.S.; Lai, O.M.; Ariff, A.B. Optimization of conditions for the single step IMAC purification of miraculin from Synsepalum dulcificum. *Food Chem.* **2015**, *181*, 19–24. [CrossRef] [PubMed]
122. Amiri, S.; Mehrnia, M.R.; Sobhanifard, S.; Roudsari, F.P.; Hosseini, S. Evaluation of agarose-entrapped magnetic nanoparticles influence on protein adsorption isotherm and kinetics using nickel-iminodiacetic acid ligand. *Sep. Purif. Technol.* **2017**, *188*, 423–430. [CrossRef]
123. Tian, F.; Yang, L.; Lv, F.; Zhou, P. Modeling and prediction of retention behavior of histidine-containing peptides in immobilized metal-affinity chromatography. *J. Sep. Sci.* **2009**, *32*, 2159–2169. [CrossRef]
124. Sidenius, U.; Farver, O.; Jøns, O.; Gammelgaard, B. Comparison of different transition metal ions for immobilized metal affinity chromatography of selenoprotein P from human plasma. *J. Chromatogr. B: Biomed. Sci. Appl.* **1999**, *735*, 85–91. [CrossRef]
125. Caetano-Silva, M.E.; Bertoldo-Pacheco, M.T.; Paes-Leme, A.F.; Netto, F.M. Iron-binding peptides from whey protein hydrolysates: Evaluation, isolation and sequencing by LC–MS/MS. *Food Res. Int.* **2015**, *71*, 132–139. [CrossRef]
126. Chen, W.-Y.; Wu, C.-F.; Liu, C.-C. Interactions of Imidazole and Proteins with Immobilized Cu(II) Ions: Effects of Structure, Salt Concentration, and pH in Affinity and Binding Capacity. *J. Colloid Interface Sci.* **1996**, *180*, 135–143. [CrossRef]
127. Hansen, P.; Lindeberg, G. Purification of tryptophan containing synthetic peptides by selective binding of the α-amino group to immobilised metal ions. *J. Chromatogr. A* **1994**, *662*, 235–241. [CrossRef]
128. Knecht, S.; Ricklin, D.; Eberle, A.N.; Ernst, B. Oligohis-tags: Mechanisms of binding to Ni2+-NTA surfaces. *J. Mol. Recognit.* **2009**, *22*, 270–279. [CrossRef]
129. Blanco-Canosa, J.B.; Wu, M.; Susumu, K.; Petryayeva, E.; Jennings, T.L.; Dawson, P.E.; Algar, W.R.; Medintz, I.L. Recent progress in the bioconjugation of quantum dots. *Co-ord. Chem. Rev.* **2014**, *263–264*, 101–137. [CrossRef]
130. Aljawish, A.; Chevalot, I.; Madad, N.; Paris, C.; Muniglia, L. Laccase mediated-synthesis of hydroxycinnamoyl-peptide from ferulic acid and carnosine. *J. Biotechnol.* **2016**, *227*, 83–93. [CrossRef] [PubMed]
131. Cuajungco, M.P.; Fagét, K.Y.; Huang, X.; Tanzi, R.E.; Bush, A.I. Metal Chelation as a Potential Therapy for Alzheimer's Disease. *Ann. N. Y. Acad. Sci.* **2006**, *920*, 292–304. [CrossRef]
132. Robert, A.; Liu, Y.; Nguyen, M.; Meunier, B. Regulation of Copper and Iron Homeostasis by Metal Chelators: A Possible Chemotherapy for Alzheimer's Disease. *Accounts Chem. Res.* **2015**, *48*, 1332–1339. [CrossRef]
133. Oshima, T.; Tachiyama, H.; Kanemaru, K.; Ohe, K.; Baba, Y. Adsorption and concentration of histidine-containing dipeptides using divalent transition metals immobilized on a chelating resin. *Sep. Purif. Technol.* **2009**, *70*, 79–86. [CrossRef]

134. Chandrudu, S.; Simerska, P.; Toth, I. Chemical Methods for Peptide and Protein Production. *Molecules* **2013**, *18*, 4373–4388. [CrossRef]
135. De Luca, C.; Felletti, S.; Macis, M.; Cabri, W.; Lievore, G.; Chenet, T.; Pasti, L.; Morbidelli, M.; Cavazzini, A.; Catani, M.; et al. Modeling the nonlinear behavior of a bioactive peptide in reversed-phase gradient elution chromatography. *J. Chromatogr. A* **2019**, *1616*, 460789. [CrossRef]
136. Merrifield, R.B. Solid Phase Peptide Synthesis. I. The Synthesis of a Tetrapeptide. *J. Am. Chem. Soc.* **1963**, *85*, 2149–2154. [CrossRef]
137. Coin, I.; Beyermann, M.; Bienert, M. Solid-phase peptide synthesis: From standard procedures to the synthesis of difficult sequences. *Nat. Protoc.* **2007**, *2*, 3247–3256. [CrossRef] [PubMed]
138. Bernaudat, F.; Bülow, L. Rapid evaluation of nickel binding properties of His-tagged lactate dehydrogenases using surface plasmon resonance. *J. Chromatogr. A* **2005**, *1066*, 219–224. [CrossRef]
139. Abe, Y.; Hiasa, K.; Hirata, I.; Okazaki, Y.; Nogami, K.; Mizumachi, W.; Yoshida, Y.; Suzuki, K.; Okazaki, M.; Akagawa, Y. Detection of synthetic RGDS(PO3H2)PA peptide adsorption using a titanium surface plasmon resonance biosensor. *J. Mater. Sci. Mater. Electron.* **2011**, *22*, 657–661. [CrossRef] [PubMed]
140. Fischer, M.; Leech, A.P.; Hubbard, R.E. Comparative Assessment of Different Histidine-Tags for Immobilization of Protein onto Surface Plasmon Resonance Sensorchips. *Anal. Chem.* **2011**, *83*, 1800–1807. [CrossRef]
141. Oshannessy, D.; Brighamburke, M.; Soneson, K.; Hensley, P.; Brooks, I. Determination of Rate and Equilibrium Binding Constants for Macromolecular Interactions Using Surface Plasmon Resonance: Use of Nonlinear Least Squares Analysis Methods. *Anal. Biochem.* **1993**, *212*, 457–468. [CrossRef]
142. Dupont, D.; Johansson, A.; Marchin, S.; Rolet-Repecaud, O.; Marchesseau, S.; Leonil, J. Topography of the Casein Micelle Surface by Surface Plasmon Resonance (SPR) Using a Selection of Specific Monoclonal Antibodies. *J. Agric. Food Chem.* **2011**, *59*, 8375–8384. [CrossRef]
143. Qu, J.-H.; Leirs, K.; Escudero, R.; Strmšek, Ž.; Jerala, R.; Spasic, D.; Lammertyn, J. Novel Regeneration Approach for Creating Reusable FO-SPR Probes with NTA Surface Chemistry. *Nanomaterials* **2021**, *11*, 186. [CrossRef]
144. Hochuli, E.; Döbeli, H.; Schacher, A. New metal chelate adsorbent selective for proteins and peptides containing neighbouring histidine residues. *J. Chromatogr. A* **1987**, *411*, 177–184. [CrossRef]
145. Nieba, L.; Nieba-Axmann, S.E.; Persson, A.; Hämäläinen, M.; Edebratt, F.; Hansson, A.; Lidholm, J.; Magnusson, K.; Karlsson, Å.F.; Plückthun, A. BIACORE Analysis of Histidine-Tagged Proteins Using a Chelating NTA Sensor Chip. *Anal. Biochem.* **1997**, *252*, 217–228. [CrossRef]
146. Qu, J.-H.; Horta, S.; Delport, F.; Sillen, M.; Geukens, N.; Sun, D.-W.; Vanhoorelbeke, K.; Declerck, P.; Lammertyn, J.; Spasic, D. Expanding a Portfolio of (FO-) SPR Surface Chemistries with the Co(III)-NTA Oriented Immobilization of His6-Tagged Bioreceptors for Applications in Complex Matrices. *ACS Sens.* **2020**, *5*, 960–969. [CrossRef]
147. Hu, W.-P.; Chang, G.-L.; Chen, S.-J.; Kuo, Y.-M. Kinetic analysis of β-amyloid peptide aggregation induced by metal ions based on surface plasmon resonance biosensing. *J. Neurosci. Methods* **2006**, *154*, 190–197. [CrossRef]
148. Achilleos, C.; Tailhardat, M.; Courtellemont, P.; Le Varlet, B.; Dupont, D. Investigation of surface plasmon resonance biosensor for skin sensitizers studies. *Toxicol. Vitr.* **2009**, *23*, 308–318. [CrossRef] [PubMed]
149. Daghestani, H.N.; Day, B.W. Theory and Applications of Surface Plasmon Resonance, Resonant Mirror, Resonant Waveguide Grating, and Dual Polarization Interferometry Biosensors. *Sensors* **2010**, *10*, 9630–9646. [CrossRef]
150. Akduman, B.; Uygun, M.; Uygun, D.A.; Antalík, M. Fe_3O_4 magnetic core coated by silver and functionalized with N-acetyl cysteine as novel nanoparticles in ferritin adsorption. *J. Nanoparticle Res.* **2013**, *15*, 1–10. [CrossRef]
151. Nguyen, H.H.; Park, J.; Kang, S.; Kim, M. Surface Plasmon Resonance: A Versatile Technique for Biosensor Applications. *Sensors* **2015**, *15*, 10481–10510. [CrossRef]
152. Wang, X.; Liu, G.; Zhang, G. Effect of Surface Wettability on Ion-Specific Protein Adsorption. *Langmuir* **2012**, *28*, 14642–14653. [CrossRef] [PubMed]
153. Li, Y.-J.; Bi, L.-J.; Zhang, X.-E.; Zhou, Y.-F.; Zhang, J.-B.; Chen, Y.-Y.; Li, W.; Zhang, Z.-P. Reversible immobilization of proteins with streptavidin affinity tags on a surface plasmon resonance biosensor chip. *Anal. Bioanal. Chem.* **2006**, *386*, 1321–1326. [CrossRef] [PubMed]
154. Drake, A.W.; Klakamp, S.L. A strategic and systematic approach for the determination of biosensor regeneration conditions. *J. Immunol. Methods* **2011**, *371*, 165–169. [CrossRef] [PubMed]
155. Andersson, P.O.; Lundquist, M.; Tegler, L.; Börjegren, S.; Baltzer, L.; Österlund, L. A Novel ATR-FTIR Approach for Characterisation and Identification of Ex Situ Immobilised Species. *ChemPhysChem* **2007**, *8*, 712–722. [CrossRef]
156. Millhauser, G.L. Copper and the Prion Protein: Methods, Structures, Function, and Disease. *Annu. Rev. Phys. Chem.* **2007**, *58*, 299–320. [CrossRef]
157. Kogelberg, H.; Miranda, E.; Burnet, J.; Ellison, D.; Tolner, B.; Foster, J.; Picón, C.; Thomas, G.J.; Meyer, T.; Marshall, J.F.; et al. Generation and Characterization of a Diabody Targeting the αvβ6 Integrin. *PLoS ONE* **2013**, *8*, e73260. [CrossRef] [PubMed]
158. Jin, J.; Wang, C.; Tao, Y.; Tan, Y.; Yang, D.; Gu, Y.; Deng, H.; Bai, Y.; Lü, H.; Wan, Y.; et al. Determination of 3-nitrotyrosine in human urine samples by surface plasmon resonance immunoassay. *Sensors Actuators B Chem.* **2011**, *153*, 164–169. [CrossRef]
159. Singh, P. SPR Biosensors: Historical Perspectives and Current Challenges. *Sensors Actuators B Chem.* **2016**, *229*, 110–130. [CrossRef]

160. Muhr, L.; Pontvianne, S.; Selmeczi, K.; Paris, C.; Boschi-Muller, S.; Canabady-Rochelle, L. Chromatographic separation simulation of metal-chelating peptides from surface plasmon resonance binding parameters. *J. Sep. Sci.* **2020**, *43*, 2031–2041. [CrossRef] [PubMed]
161. Gerontas, S.; Asplund, M.; Hjorth, R.; Bracewell, D.G. Integration of scale-down experimentation and general rate modelling to predict manufacturing scale chromatographic separations. *J. Chromatogr. A* **2010**, *1217*, 6917–6926. [CrossRef] [PubMed]
162. Yon, R.J.; Kyprianou, P.; Winzor, D.J.; Smith, V.R.; Fearnley, I.M.; Walker, J.E.; Stevens, F.J.; Schiffer, M. Sensitivity and other factors affecting biospecific desorption in chromatography of proteins. A study by computer simulation. *Biochem. J.* **1980**, *185*, 211–216. [CrossRef]
163. Schmidt-Traub, H. (Ed.) *Preparative Chromatography of Fine Chemicals and Pharmaceutical Agents*; Wiley-VCH: Weinheim, Germany, 2005.
164. Bellot, J.; Condoret, J. Liquid chromatography modelling: A review. *Process Biochem.* **1991**, *26*, 363–376. [CrossRef]
165. Du, H.; Zhang, X.; Wang, J.; Yao, X.; Hu, Z. Novel approaches to predict the retention of histidine-containing peptides in immobilized metal-affinity chromatography. *Proteomics* **2008**, *8*, 2185–2195. [CrossRef]
166. Harscoat-Schiavo, C.; Raminosoa, F.; Ronat-Heit, E.; Vanderesse, R.; Marc, I. Modeling the separation of small peptides by cation-exchange chromatography: Liquid Chromatography. *J. Sep. Sci.* **2010**, *33*, 2447–2457. [CrossRef]
167. Badgett, M.J.; Boyes, B.; Orlando, R. Peptide retention prediction using hydrophilic interaction liquid chromatography coupled to mass spectrometry. *J. Chromatogr. A* **2018**, *1537*, 58–65. [CrossRef] [PubMed]
168. Le Maux, S.; Nongonierma, A.B.; FitzGerald, R.J. Improved short peptide identification using HILIC–MS/MS: Retention time prediction model based on the impact of amino acid position in the peptide sequence. *Food Chem.* **2015**, *173*, 847–854. [CrossRef] [PubMed]
169. Yoshida, T. Calculation of peptide retention coefficients in normal-phase liquid chromatography. *J. Chromatogr. A* **1998**, *808*, 105–112. [CrossRef]
170. Guo, D.; Mant, C.T.; Taneja, A.K.; Hodges, R.S. Prediction of peptide retention times in reversed-phase high-performance liquid chromatography II. Correlation of observed and predicted peptide retention times factors and influencing the retention times of peptides. *J. Chromatogr. A* **1986**, *359*, 519–532. [CrossRef]
171. Boateng, B.O.; Fever, M.; Edwards, D.; Petersson, P.; Euerby, M.R.; Sutcliffe, O.B. Chromatographic retention behaviour, modelling and optimization of a UHPLC-UV separation of the regioisomers of the Novel Psychoactive Substance (NPS) methoxphenidine (MXP). *J. Pharm. Biomed. Anal.* **2018**, *153*, 238–247. [CrossRef]
172. García-Álvarez-Coque, M.; Torres-Lapasió, J.; Baeza-Baeza, J. Models and objective functions for the optimisation of selectivity in reversed-phase liquid chromatography. *Anal. Chim. Acta* **2006**, *579*, 125–145. [CrossRef]
173. Jandera, P. Can the theory of gradient liquid chromatography be useful in solving practical problems? *J. Chromatogr. A* **2006**, *1126*, 195–218. [CrossRef]
174. Ng, B.K.; Tan, T.T.; Shellie, R.A.; Dicinoski, G.W.; Haddad, P.R. Computer-assisted simulation and optimisation of retention in ion chromatography. *Trac Trends Anal. Chem.* **2016**, *80*, 625–635. [CrossRef]
175. Pfeifer, N.; Leinenbach, A.; Huber, C.G.; Kohlbacher, O. Statistical learning of peptide retention behavior in chromatographic separations: A new kernel-based approach for computational proteomics. *BMC Bioinform.* **2007**, *8*, 468. [CrossRef]
176. Petritis, K.; Kangas, L.J.; Ferguson, P.L.; Anderson, G.A.; Paša-Tolić, L.; Lipton, M.S.; Auberry, K.J.; Strittmatter, E.F.; Shen, Y.; Zhao, R.; et al. Use of Artificial Neural Networks for the Accurate Prediction of Peptide Liquid Chromatography Elution Times in Proteome Analyses. *Anal. Chem.* **2003**, *75*, 1039–1048. [CrossRef]
177. Sharma, S.; Agarwal, G.P. Interactions of Proteins with Immobilized Metal Ions: A Comparative Analysis Using Various Isotherm Models. *Anal. Biochem.* **2001**, *288*, 126–140. [CrossRef] [PubMed]
178. Yang, Y.-H.; Wu, T.-T.; Suen, S.-Y.; Lin, S.-C. Equilibrium adsorption of poly(His)-tagged proteins on immobilized metal affinity chromatographic adsorbents. *Biochem. Eng. J.* **2011**, *54*, 1–9. [CrossRef]
179. Tercinier, L.; Ye, A.; Anema, S.; Singh, A.; Singh, H. Adsorption of milk proteins on to calcium phosphate particles. *J. Colloid Interface Sci.* **2013**, *394*, 458–466. [CrossRef]
180. Latour, R.A. The langmuir isotherm: A commonly applied but misleading approach for the analysis of protein adsorption behavior. *J. Biomed. Mater. Res. Part A* **2014**, *103*, 949–958. [CrossRef]
181. Lan, Q.; Bassi, A.S.; Zhu, J.-X.; Margaritis, A. A modified Langmuir model for the prediction of the effects of ionic strength on the equilibrium characteristics of protein adsorption onto ion exchange/affinity adsorbents. *Chem. Eng. J.* **2001**, *81*, 179–186. [CrossRef]
182. Shekhawat, L.K.; Chandak, M.; Rathore, A.S. Mechanistic modeling of hydrophobic interaction chromatography for monoclonal antibody purification: Process optimization in the quality by design paradigm. *J. Chem. Technol. Biotechnol.* **2017**, *92*, 2527–2537. [CrossRef]
183. Ghosal, P.S.; Gupta, A.K. Determination of thermodynamic parameters from Langmuir isotherm constant-revisited. *J. Mol. Liq.* **2016**, *225*, 137–146. [CrossRef]
184. Epstein, J.; Michael, J.; Mandona, C.; Marques, F.; Dias-Cabral, A.; Thrash, M. Modeling Langmuir isotherms with the Gillespie stochastic algorithm. *J. Chromatogr. A* **2015**, *1380*, 81–87. [CrossRef]
185. Vunnum, S.; Gallant, S.R.; Kim, Y.J.; Cramer, S.M. Immobilized metal affinity chromatography: Modeling of nonlinear multicomponent equilibrium. *Chem. Eng. Sci.* **1995**, *50*, 1785–1803. [CrossRef]

186. Arnell, R.; Ferraz, N.; Fornstedt, T. Analytical Characterization of Chiral Drug−Protein Interactions: Comparison between the Optical Biosensor (Surface Plasmon Resonance) Assay and the HPLC Perturbation Method. *Anal. Chem.* **2006**, *78*, 1682–1689. [CrossRef]
187. Vicente, T.; Mota, J.P.; Peixoto, C.; Alves, P.; Carrondo, M.J. Modeling protein binding and elution over a chromatographic surface probed by surface plasmon resonance. *J. Chromatogr. A* **2010**, *1217*, 2032–2041. [CrossRef] [PubMed]
188. Vicente, T.; Mota, J.P.; Peixoto, C.; Alves, P.; Carrondo, M.J. Analysis of adsorption of a baculovirus bioreaction bulk on an ion-exchange surface by surface plasmon resonance. *J. Biotechnol.* **2010**, *148*, 171–181. [CrossRef] [PubMed]
189. Hahn, T.; Sommer, A.; Osberghaus, A.; Heuveline, V.; Hubbuch, J. Adjoint-based estimation and optimization for column liquid chromatography models. *Comput. Chem. Eng.* **2014**, *64*, 41–54. [CrossRef]
190. Gritti, F.; Guiochon, G. Adsorption mechanism of acids and bases in reversed-phase liquid chromatography in weak buffered mobile phases designed for liquid chromatography/mass spectrometry. *J. Chromatogr. A* **2009**, *1216*, 1776–1788. [CrossRef] [PubMed]
191. Jakobsson, N.; Degerman, M.; Stenborg, E.; Nilsson, B. Model based robustness analysis of an ion-exchange chromatography step. *J. Chromatogr. A* **2007**, *1138*, 109–119. [CrossRef]
192. Close, E.J.; Salm, J.R.; Bracewell, D.G.; Sorensen, E. Modelling of industrial biopharmaceutical multicomponent chromatography. *Chem. Eng. Res. Des.* **2014**, *92*, 1304–1314. [CrossRef]
193. Heuer, C.; Seidel-Morgenstern, A.; Hugo, P. Experimental investigation and modelling of closed-loop recycling in preparative chromatography. *Chem. Eng. Sci.* **1995**, *50*, 1115–1127. [CrossRef]
194. Guélat, B.; Ströhlein, G.; Lattuada, M.; Delegrange, L.; Valax, P.; Morbidelli, M. Simulation model for overloaded monoclonal antibody variants separations in ion-exchange chromatography. *J. Chromatogr. A* **2012**, *1253*, 32–43. [CrossRef]
195. Glueckauf, E. Theory of chromatography. VII. The general theory of two solutes following non-linear isotherms. *Discuss. Faraday Soc.* **1949**, *7*, 12–25. [CrossRef]
196. Rhee, H.-K.; Tondeur, D.; Rodrigues, A.E. *Equilibrium Theory of Multicomponent Chromatography in Percolation Processes: Theory and Application*; Springer: Berlin/Heidelberg, Germany, 1985; pp. 285–328.
197. Rhee, H.K.; Amundson, N.R. On the Theory of Multicomponent Chromatography. Philosophical transactions of the Royal Society of London. *Ser. A Math. Phys. Sci.* **1970**, *267*, 419–455.
198. Carta, G.; Jungbauer, A. *Protein Chromatography: Process Development and Scale-Up*; Wiley-VCH: Weinheim, Germany, 2010.
199. Ng, C.K.; Osuna-Sanchez, H.; Valéry, E.; Sørensen, E.; Bracewell, D.G. Design of high productivity antibody capture by protein A chromatography using an integrated experimental and modeling approach. *J. Chromatogr. B* **2012**, *899*, 116–126. [CrossRef] [PubMed]
200. Ziomek, G.; Antos, D.; Tobiska, L.; Seidel-Morgenstern, A. Comparison of possible arrangements of five identical columns in preparative chromatography. *J. Chromatogr. A* **2006**, *1116*, 179–188. [CrossRef] [PubMed]